THE JOURNAL OF BIOLOGICAL CHEMISTRY VOL. 283, NO. 4, pp. 2231–2245, January 25, 2008

Quercetin 3-Glucoside Protects Neuroblastoma (SH-SY5Y) Cells *in Vitro* against Oxidative Damage by Inducing Sterol Regulatory Element-binding Protein-2-mediated Cholesterol Biosynthesis*[S]

Received for publication, April 30, 2007, and in revised form, November 20, 2007 Published, JBC Papers in Press, November 20, 2007, DOI 10.1074/jbc.M703583200

Ramani Soundararajan[‡1], Alexander D. Wishart[‡2], H. P. Vasantha Rupasinghe[§], Mayi Arcellana-Panlilio[¶], Carolanne M. Nelson[‖], Michael Mayne[**], and George S. Robertson[‡‡3]

*From the [‡]Department of Pharmacology and [‡‡]Departments of Psychiatry and Pharmacology, Dalhousie University, Halifax, Nova Scotia B3H 1X5, Canada, the [§]Department of Environmental Sciences, Nova Scotia Agricultural College, Truro, Nova Scotia B2N 5E3, Canada, the [¶]Department of Biochemistry and Molecular Biology, University of Calgary, HM 393b-3330 Hospital Drive, N.W., Calgary, Alberta T2N 4N1, Canada, the [‖]Department of Family and Nutritional Sciences, University of Prince Edward Island, Charlottetown, Prince Edward Island C1A 4P3, Canada and the **Institute for Nutrisciences and Health, National Research Council of Canada, Charlottetown, Prince Edward Island C1A 5T1, Canada*

The flavonoid quercetin 3-glucoside (Q3G) protected SH-SY5Y, HEK293, and MCF-7 cells against hydrogen peroxide-induced oxidative stress. cDNA microarray studies suggested that Q3G-pretreated cells subjected to oxidative stress up-regulate the expression of genes associated with lipid and cholesterol biosynthesis. Q3G pretreatment elevated both the expression and activation of sterol regulatory element-binding protein-2 (SREBP-2) only in SH-SY5Y cells subjected to oxidative stress. Inhibition of SREBP-2 expression by small interfering RNA or small molecule inhibitors of 2,3-oxidosqualene:lanosterol cyclase or HMG-CoA reductase blocked Q3G-mediated cytoprotection in SH-SY5Y cells. By contrast, Q3G did not protect either HEK293 or MCF-7 cells via this signaling pathway. Moreover, the addition of isopentenyl pyrophosphate rescued SH-SY5Y cells from the inhibitory effect of HMG-CoA reductase inhibition. Last, Q3G pretreatment enhanced the incorporation of [^{14}C]acetate into [^{14}C]cholesterol in SH-SY5Y cells under oxidative stress. Taken together, these studies suggest a novel mechanism for flavonoid-induced cytoprotection in SH-SY5Y cells involving SREBP-2-mediated sterol synthesis that decreases lipid peroxidation by maintaining membrane integrity in the presence of oxidative stress.

Cholesterol, phospholipids, and sphingolipids are major structural components of the eukaryotic plasma membrane that play an essential role in maintaining membrane integrity. In the hydrophobic region of the membrane bilayer, sterols fill the spaces created by the acyl chains of phospholipids, thereby conferring rigidity and decreasing permeability (1). The biological function of membrane proteins is influenced by cholesterol in a number of ways (2). Cholesterol levels can regulate the activity of enzymes involved in the biosynthetic pathway of this lipid and form membrane rafts that participate in signal transduction (3). The importance of raft-associated cholesterol in cancer cell proliferation, migration, and cell survival has been well documented (4).

Cholesterol is derived endogenously from acetyl-CoA and exogenously by low density lipoprotein (LDL)[4] receptor-mediated uptake of plasma LDL (5). The synthesis and uptake of cholesterol are regulated by the transcription factors sterol regulatory element-binding proteins SREBPs (6). Alternate splicing of SREBP-1 gives rise to SREBP-1a and SREBP-1c, which activates genes involved in fatty acid metabolism, whereas SREBP-2 activates genes critical to cholesterol synthesis (6). SREBP-2 is synthesized as a 125-kDa precursor protein. When cholesterol levels are low, SREBP cleavage-activating protein (SCAP) escorts SREBP-2 from the endoplasmic reticulum to Golgi, where SREBP-2 is proteolytically cleaved by proteases into a mature form (65 kDa) that translocates to the nucleus and binds to the sterol regulatory element, triggering the transcrip-

* This work was supported in part by grants from Atlantic Canada Opportunities Agency-Atlantic Innovation Funds (to C. M. N. and G. S. R.). The costs of publication of this article were defrayed in part by the payment of page charges. This article must therefore be hereby marked "*advertisement*" in accordance with 18 U.S.C. Section 1734 solely to indicate this fact.

The microarray data has been deposited to the NCBI gene expression and hybridization array repository (GEO; http://www.ncbi.nlm.nih.gov/geo), and GEO accession numbers are GSE6199, GSE6200, GSM143163, GSM143243, GSM143247, GSM143248, GSM143249, GSM143250, GSM143251, GSM143252, GSM143253, GSM143254, GSM143255, GSM143256, GSM143257, GSM143258, GSM143259, and GSM143260.

[S] The on-line version of this article (available at http://www.jbc.org) contains supplemental Figs. 1–5.

[1] Supported by a Postdoctoral fellowship from the Department of Family and Nutritional Sciences, University of Prince Edward Island.

[2] Supported by a studentship from Vaccinium Technologies Inc.

[3] To whom correspondence should be addressed: Dept. of Psychiatry and Pharmacology, Sir Charles Tupper Medical Bldg., Dalhousie University, 5850 College St., Halifax, Nova Scotia B3H 1X5, Canada. Tel.: 902-494-1528; Fax: 902-494-1388; E-mail: George.Robertson@dal.ca.

[4] The abbreviations used are: LDL, low density lipoprotein; Q3G, quercetin 3-glucoside; Q dihydrate, quercetin dihydrate; MTT, (3-[4,5-dimethylthiazole-2-yl]-2,5-diphenyltetrazolium bromide); SCD1, stearoyl-CoA-desaturase 1; HMG-CoA reductase, 3-hydroxy-3-methylglutaryl-coenzyme A reductase; SREBP, sterol regulatory element-binding protein; SCAP, SREBP cleavage-activating protein; ROS, reactive oxygen species; siRNA, small interfering RNA; OSCi, oxidosqualene:lanosterol cyclase inhibitor; LDLr, LDL receptor; PBS, phosphate-buffered saline; ELISA, enzyme-linked immunosorbent assay; LDH, lactate dehydrogenase; TUNEL, terminal deoxynucleotidyltransferase-mediated deoxyuridine triphosphate nick end *in situ* labeling; SAMF, Southern Alberta Microarray Facility; RT, reverse transcription; GAPDH, glyceraldehyde-3-phosphate dehydrogenase; tBHQ, *tert*-butylhydroquinone; SAM, Significance Analysis of Microarray; qRT, quantitative RT; IPP, isopentenyl pyrophosphate.

tion of genes necessary for cholesterol synthesis (7). If cholesterol levels exceed cellular demands, the SCAP·SREBP complex is sequestered in the endoplasmic reticulum by the insulin-induced gene product known as Insig-1 (8). Recently, plasma membrane compartments rich in cholesterol have been reported to participate in cell survival pathways that reduce the injurious oxidative stress (9).

Oxidative stress is a pathophysiological state that occurs when free radicals and reactive oxygen species (ROS) exceed the ability of antioxidant small molecules and proteins to neutralize them (10). Oxidative stress has been implicated in a number of pathological conditions (11–13). The injurious events triggered by ROS are thought to include lipid peroxidation (14), ion channel modification, DNA damage, and protein oxidation (15). Lipids are susceptible to oxidative damage because of their high degree of unsaturation and abundance in cell membranes. Neurons in the central nervous system are highly susceptible to oxidative stress due to their high rate of aerobic metabolism, presence of catalysts such as heavy metals that generate free radicals, excitotoxic amino acids, and low levels of antioxidants (16–18). Hence, we used the neuroblastoma SH-SY5Y cells as an *in vitro* model to assess the effects of oxidative stress on a neuronal-like cell line. Oxidative stress generated by free radicals is counteracted by sophisticated antioxidant defense systems (19, 20); however, the excessive production of ROS during pathological conditions may overwhelm endogenous antioxidant defenses resulting in tissue injury. Antioxidants derived from dietary sources have been shown to reduce oxidative tissue damage (21).

Among the most potent dietary free radical scavengers identified to date are a class of polyphenolic compounds known as flavonoids found in wine, fruits, vegetables, and teas (21). Epidemiological data suggest that apple flavonoids reduce the risk of cancer, cardiovascular disease, and neurological disorders (22). Quercetin and its glycoside derivatives are the most abundantly consumed flavonoids in the diet, reaching levels of 30–40 mg/day (23). Flavonoids are known to scavenge free radicals, inhibit a variety of kinases, reduce lipid peroxidation, inhibit apoptosis, prevent platelet aggregation, and exhibit antiproliferative effects (24–26). Several flavonoids have been documented to cross the blood-brain barrier and to protect neurons from cell death in both *in vitro* and *in vivo* models of neurodegenerative diseases (27–29).

In the present study, we first demonstrate cytoprotective effects of Q3G against hydrogen peroxide injury associated with oxidative stress in SH-SY5Y cells. In order to determine if Q3G-mediated cytoprotection against oxidative stress is applicable to other cell lines that are not neuronal in origin, we also determined that Q3G protects the human embryonic kidney cell line HEK293 and the human breast cancer cell line MCF-7 from oxidative injury. Then using cDNA microarrays to profile changes in gene expression associated with Q3G-mediated cytoprotection in SH-SY5Y cells, we report that only in cells pretreated with Q3G and then subjected to oxidative stress was the expression of numerous genes implicated in cholesterol biosynthesis elevated. Since the transcriptional regulating factor SREBP-2 plays a critical role in this biosynthesis and was activated in cells pretreated with Q3G and subjected to oxidative stress, cholesterol synthesis was blocked using siRNA technology to knock down SREBP-2 expression and chemical inhibitors to block the biosynthetic enzymes HMG-CoA reductase and 2,3-oxidosqualene:lanosterol cyclase (OSC). We show using these approaches that Q3G-induced *de novo* cholesterol synthesis plays a pivotal role in the cytoprotective effects of this flavonoid in SH-SY-5Y cells perhaps by enhancing membrane integrity that resists lipid peroxidation in the face of oxidative stress.

EXPERIMENTAL PROCEDURES

Materials—Q3G was purchased from ChromaDex Inc. (Santa Ana, CA). The purity of Q3G was greater than 99.0% as determined by high pressure liquid chromatography/UV, NMR, and mass spectrometry. Caspase-3-cleaved spectrin antibody was generously provided by Dr. Donald Nicholson (Merck). Oxidosqualene:lanosterol cyclase inhibitor (OSCi), designated as RO0714565 (IC_{50} = 10 nM), was generously provided by Hoffman-La Roche (Pharmaceutical Division, Basal, Switzerland). [^{14}C]Acetate, sodium salt (55 mCi/mmol; 1.66–2.22 GBq/mmol), and [^{14}C]cholesterol (58.0 mCi/mmol; 2.15 GBq/mmol) were purchased from PerkinElmer and Amersham Biosciences, respectively. Cell culture reagents were obtained from Hyclone. All other chemicals and reagents were purchased from Sigma.

Plasmids—The LDLp-588luc and TK-LXRE3-luc plasmids were gifts from Dr. D. S. Ory (30). LDLp-588luc contains the human LDL receptor (LDLr) promoter upstream of the luciferase reporter gene. The β-galactosidase construct was generously provided by Dr. C. Sinal (Department of Pharmacology, Dalhousie University, Halifax, Canada).

Cell Culture—The human neuroblastoma cells (SH-SY5Y), human embryonic kidney cells (HEK293), and human breast cancer cells (MCF-7) were obtained from the American Type Culture Collection. SH-SY5Y, MCF-7, and HEK293 cells were grown in Dulbecco's modified Eagle's medium supplemented with 10% serum (10% fetal bovine serum for SH-SY5Y and MCF-7 cells; 10% horse serum for HEK293 cells), 2 mM L-glutamine, 1 mM sodium pyruvate, penicillin (100 units/ml), and streptomycin (100 μg/ml) at 37 °C in a humidified atmosphere of 5% CO_2. These cell lines were seeded at an initial density of 5×10^5 cells/ml in a 75-cm^2 flask and passaged every third day. SH-SY5Y cells doubled every 48 h, whereas HEK293 and MCF-7 cells doubled every 24 h.

3-(4,5-Dimethylthiazol-2-yl)-2,5-diphenyltetrazolium Bromide (MTT) Assay—Cell viability was determined using the MTT assay (supplemental Fig. 1, *A–D*). SH-SY5Y, HEK293, and MCF-7 cells were seeded in a 96-well plate at a density of 1×10^4 cells/100 μl and treated with varying concentrations of Q3G (0.01–100 μM), quercetin dihydrate (0.01–100 μM), or Me_2SO vehicle for 6 or 18 h. Following a rinse in PBS, the cells were subjected to an H_2O_2 insult (500 μM for 15 min for SH-SY5Y cells, 500 μM for 3 h for HEK293 cells, and 800 μM for 24 h for MCF-7 cells, respectively). After several washes, the cells were maintained in the growth medium for 18 h. The cells were then incubated with 0.5 mg/ml MTT (Sigma) at 37 °C for 4 h. The formazan crystals generated by viable mitochondrial succinate dehydrogenase from MTT were extracted using an

equal volume of the solubilizing buffer (0.01 N HCl and 10% SDS). Absorbance was measured at 562 nm in an ELx800$_{uv}$ microplate reader (Bio-tek Instruments, Inc.). The resultant data were expressed as the percentage of viable cells relative to untreated controls.

Cell Death ELISA—A cell death ELISA kit that detects cytoplasmic histone-associated DNA fragments in cell lysates was used to assess cell death according to the manufacturer's instructions (Roche Applied Science). Briefly, cells were seeded in a 24-well plate at a density of 5×10^4 cells/500 μl and treated with Q3G (10 μM) or *tert*-butylhydroquinone (tBHQ) (5 μM) for 18 h. Following a rinse in PBS, the cells were subjected to an H_2O_2 insult (500 μM for 15 min). After several washes, the cells were maintained in the growth medium for 18 h. The positive control was prepared according to the manufacturer's instructions (Roche Applied Science). Absorbance was read at 405 nm using an ELx800$_{uv}$ microplate reader (Bio-tek Instruments). DNA fragmentation was expressed as an enrichment factor, a measure of specific enrichment of mono- and oligonucleosomes in the cell lysates. The enrichment factor was calculated as a ratio of the absorbance of the test sample to that of the untreated control.

Cytotoxicity Assay—Cell membrane integrity was assayed by measuring the release of lactate dehydrogenase (LDH) using the CytoTox nonradioactive kit (Promega). A positive control was prepared according to the manufacturer's instructions (Promega). Cells were plated in a 96-well plate at a density of 1×10^4 cells/100 μl in phenol red-free Dulbecco's modified Eagle's medium supplemented with 5% fetal bovine serum, 1 mM sodium pyruvate, and 2 mM L-glutamine. After 18 h, cells were incubated with Q3G (10 μM) for 6 h. The medium was replaced, and cells were subjected to an H_2O_2 insult (500 μM for 15 min). After washing, the cells were incubated with mevastatin (1 μM) for 18 h. The cells were then centrifuged at 250 $\times$ *g* for 4 min, and 50 μl of medium was removed from each well of the plate and transferred to another 96-well plate. An equal volume of substrate solution containing 2-(*p*-iodophenyl)-3-(*p*-nitrophenyl)-5-phenyl-2H-tetrazolium chloride salts and diaphorase was added to the medium and incubated in the dark at room temperature for 30 min. The reaction was terminated by the addition of 50 μl of stop solution to each of the wells. Absorbance was measured at 490 nm using an ELx800$_{uv}$ microplate reader (Bio-tek Instruments). The background value was subtracted, and the result was expressed as a percentage of LDH release compared with the positive control.

Terminal Deoxynucleotidyltransferase-mediated Deoxyuridine Triphosphate Nick End in Situ Labeling (TUNEL)—TUNEL labeling was performed to detect damaged cells by labeling the nicked end of DNA with terminal deoxynucleotidyltransferase using the Apo Tag kit as per the manufacturer's instructions (Roche Applied Science) (supplemental Fig. 2*A*). Cells seeded on a coverslip in a 24-well plate at a density of 5×10^4 cells/500 μl were treated with Q3G (10 μM) for 18 h. Following a rinse in PBS, the cells were subjected to H_2O_2 insult (500 μM for 15 min). After several washes, the cells were maintained in growth medium for 18 h. We included both a positive control (cells treated with 10 units of DNase for 20 min) and a negative control (cells not treated with terminal deoxynucleotidyltransferase enzyme) in the assay. TUNEL staining was then performed, and slides were mounted with DakoCytomation fluorescent mounting medium (DakoCytomation, Carpinteria, CA). The images were captured on a Zeiss inverted microscope using a Nikon camera.

Determination of ROS—ROS was measured using 5-(and 6-)carboxy-2,7-dichlorofluorescin diacetate (Molecular Probes) as substrate that is oxidized to a fluorescent product in the presence of ROS (supplemental Fig. 2*B*). Cells were seeded in a 24-well plate at a density of 5×10^5 cells/500 μl in phenol red free Dulbecco's modified Eagle's medium supplemented with 10% fetal bovine serum, 1 mM sodium pyruvate, and 2 mM L-glutamine. Cells were then incubated with Q3G, tBHQ, or vehicle (0.01 and 0.05% Me_2SO) for 18 h. Following a rinse in PBS, the cells were subjected to the H_2O_2 insult (500 μM for 15 min) and treated with 0.11 mg/ml horseradish peroxidase for 15 min. 5-(and 6-)Carboxy-2,7-dichlorofluorescin diacetate (10 μM) was added to the cells immediately after the insult and incubated at 37 °C for 15 min. Subsequently, the cells were washed with PBS and lysed in 10 mM Tris-HCl buffer containing 0.5% Tween 20. The lysates were centrifuged at 10,000 $\times$ *g* for 10 min, and the supernatant was added to an opaque 96-well plate (Costar). Fluorescence was measured using Flx800 microplate fluorescence reader (Bio-tek Instruments) with an excitation wavelength (485 nm) and an emission wavelength (528 nm). ROS was expressed as -fold induction compared with untreated cells that received no oxidative insult.

cDNA Microarray Studies—cDNA microarray studies were performed by the Southern Alberta Microarray Facility (SAMF) using human 14K microarray slides (GEO Platform accession numbers GPL3963 and GPL3964), printed at the University of Calgary. These arrays contain 13,972 70-mer oligonucleotides designed against the UniGene data base (Operon version 1.0) spotted in duplicate. For further information concerning the genes represented on these microarray chips and the microarrays used in these experiments, please see the SAMF site on the World Wide Web.

RNA Extraction—In the first experiment, SH-SY5Y cells were treated with Q3G (10 μM) or Me_2SO vehicle (0.05%) for 6 h. In a second experiment, SH-SY5Y cells were treated with Q3G (10 μM) or Me_2SO vehicle (0.05%) for 6 h and subjected to an H_2O_2 insult (500 μM for 15 min) and allowed to recover for 6 h in growth medium before RNA extraction. Total RNA was extracted using an RNeasy minicolumn (Qiagen). The integrity of total RNA was determined on a 1% formaldehyde-agarose gel, and the absorbance of RNA was measured at 260 and 280 nm using a spectrophotometer. RNA samples having a 260/280 absorbance ratio of 1.9–2.0 were subsequently used for microarray analysis.

cDNA Synthesis, Purification, and Hybridization—cDNA microarray studies were carried out by the SAMF at the University of Calgary. cDNA labeling was performed using the FairPlay Microarray Labeling Kit II (catalog number 252006; Stratagene). For the detailed protocol, please see the Web site).

Meaurement of Microarray Data and Specification—The scans were saved as image files in TIFF format and imported into QuantArray™ version 3.0 (PerkinElmer Life Sciences) microarray analysis software used for spot identification, quan-

tification, and background estimation. The quantified and imaged gpr files were then loaded into Gene Traffic Duo™ (Iobion) for microarray data management and analysis. The data were filtered to flag spots with intensities of less than 100 units, or less than twice the average background. The data were normalized according to the Lowess method resident in the Gene Traffic software (31). In order to identify genes that were differentially expressed and statistically significant, Significance Analysis of Microarray (SAM) version 2.2 software was used (available on the World Wide Web). The data set created in Gene Traffic 4.0 was analyzed by SAM using the following criteria: one class analysis, median center arrays, and 100 permutations. SAM plots (supplemental Fig. 3, *A* and *B*) and SAM tables were generated at corresponding Δ values. The number of significant genes with a -fold change greater than 1.5 and a false discovery rate of <7% were determined. These significant genes were further analyzed through Panther software (available on the World Wide Web) to delineate the potential biological processes involved (supplemental Fig. 3*C*). The pathways defined by this set of genes were analyzed using Pathway Architect (Stratagene).

Quantitative Real Time PCR—Quantitative RT-PCR was performed using the DNA Engine Opticon 2 System (MJ Research) (supplemental Figs. 4, *A–E*, and 5, *A* and *B*). Total RNA was isolated from Q3G-, Q dihydrate-, and Me_2SO-treated SH-SY5Y, HEK293, and MCF-7 cells that were subjected to oxidative stress using the RNeasy minicolumn (Qiagen). Briefly, 3 μg of DNase-treated total RNA was reverse transcribed using a First Strand cDNA synthesis kit according to the manufacturer's instructions (Superarray Incorporation Inc.). The 20-μl RT reaction mix was diluted 5-fold in RNase-free water. In order to validate up-regulated genes, cDNA from Q3G-treated cells was serially diluted 10-fold (5 points in duplicates), and the standard curve was generated for GAPDH and the genes of interest (SCD1 and HMG-CoA reductase and SREBP-2, respectively). To validate a down-regulated gene (sestrin 1), cDNA from Me_2SO-treated cells was serially diluted 10-fold (5 points in duplicates), and standard curves were generated for GAPDH and sestrin 1, respectively. A negative (no RT control) was included in all of the experiments. Triplicates of control and experimental cDNA samples were included in the experiment at an appropriate dilution. PCR master mix was prepared using an RT^2 Real-Time™ PCR kit using gene-specific primers in 25 μl/well of a 96-well plate as per the manufacturer's instructions (Superarray Incorporation Inc.). The cycling parameter included activation of Taq polymerase at 95 °C for 15 min. This step was followed by denaturation at 95 °C/15 s, annealing for SCD1 at 60 °C/30 s with the primers 5′-TACCGCTGGCACATCAACTT-3′ (sense) and 5′-TTGGAGACTTTCTTCCGGTCA-3′ (antisense) (32) (product size, 87 bp); annealing for HMG-CoA reductase at 55 °C/30 s with the primers 5′-TACCATGTCAGGGGTACGTC-3′ (sense) and 5′-CAAGCCTAGAGACATAATCATC-3′ (antisense) (33) (product size, 247 bp); annealing for sestrin 1 at 58 °C/30 s with the primers 5′-GGCAAACCATTTTGAGGAAA-3′ (sense) and 5′-ACTCCCCACTTGGAGGATCT-3′ (antisense) (PRIMER 3 software) (available on the World Wide Web) (product size, 278 bp); annealing for SREBP-2 at 62 °C/40 s with the primers 5′-CCCTTCAGTGCAACGGTCATTCAC-3′ (sense) and 5′-GATGCTCAGTGGCACTGACTCTTC-3′ (antisense), respectively (33) (product size, 401 bp) and primer extension at 72 °C/30 s for a total of 40 cycles. The GAPDH Amplimer set (Clontech) was used to amplify GAPDH (450 bp). The melting curve analysis was performed to verify the accurate amplification of target amplicon. Data analysis was performed using Opticon software version 2.02. Using the standard curve generated for SCD1, HMG-CoA reductase, SREBP-2, sestrin 1, and GAPDH, respectively, the relative -fold increase in gene expression in the Q3G-treated sample over the Me_2SO control was calculated using the comparative C_T method ($\Delta\Delta C_T$) (34) and was quantified using $2^{-\Delta\Delta C_T}$ with GAPDH as the internal control. The data were expressed as the relative -fold increase or decrease in gene expression compared with the Me_2SO control.

Lipid Peroxidation Assay—Lipid peroxidation is the method of choice for detecting phospholipid oxidation in cells either by measuring the initial products of oxidative attack, such as the lipid hydroperoxides and conjugated dienes, or by measuring the breakdown products of polyunsaturated fatty acid, namely malondialdehyde and 4-hydroxynonenal. A lipid peroxidation kit (Calbiochem) was used to measure lipid hydroperoxides generated by lipid oxidation utilizing a redox reaction with ferrous ions. The reaction of hydroperoxides with ferrous ions resulted in the generation of ferric ions that were detected using thiocyanate as a chromogen. Briefly, cells were seeded in a 6-well plate at a density of 5×10^5 cells/ml and incubated with Q3G (10 μM) or Me_2SO (0.05%) for 6 h. The cells were then rinsed with PBS and subjected to H_2O_2 insult (500 μM for 15 min). The medium was replaced, and after 6 h, the lipid hydroperoxides were extracted from the cells using Extract R-saturated methanol and deoxygenated chloroform as per the manufacturer's instructions (Calbiochem). For the lipid peroxidation assay, a standard curve was generated. Briefly, standard and test samples were diluted in deoxygenated chloroform/methanol mixture (2:1) in a reaction volume of 950 μl in a glass tube. Chromogen substrate was freshly prepared, added to the samples (50 μl), and incubated at room temperature for 5 min. A volume of 300 μl was transferred from the glass tube to a glass 96-well plate, and absorbance was read at 490 nm using an $ELx800_{uv}$ microplate reader (Bio-tek Instruments). The lipid hydroperoxides in the test sample were extrapolated from a standard curve and expressed as nM/mg of protein.

Cholesterol Assay—SH-SY5Y cells were seeded in a 6-well plate at a density of 5×10^5 cells/ml. Cells were incubated with Q3G (10 μM) or Me_2SO vehicle (0.05%) for 6 h and exposed to H_2O_2 insult (500 μM for 15 min). After washing and incubation in growth medium for 6 h, the cells were counted. A phase separation method (chloroform/methanol, 2:1) was used to extract cholesterol from 8.5×10^5 cells. The organic phase was evaporated, and the lipids were dissolved in 2-propanol. Cholesterol and cholesterol esters were measured as per the manufacturer's protocol (Biovision). The samples were diluted 1:25 in 50 μl of the cholesterol reaction buffer. An equal volume of reaction mix containing cholesterol reaction buffer, cholesterol probe, enzyme mix, and cholesterol esterase was added to the

samples and incubated in the dark for 60 min at 37 °C. Absorbance was read at 562 nm using an ELx800$_{uv}$ microplate reader (Bio-tek Instruments). The values obtained were subtracted from blank containing the reaction buffer and extrapolated from the standard curve for cholesterol. Total cellular cholesterol was expressed as μg/μl per sample.

Determination of Cholesterol Synthesis Using [^{14}C]Acetate—The *de novo* synthesis of cholesterol was determined using methodology adapted from Singh and Porter (35) with slight modifications. SH-SY5Y cells were cultured in 6-well plates at a density of 5×10^5 cells/ml and incubated with 1 μCi (37 kBq) of [^{14}C]acetate (PerkinElmer Life Sciences) for 24 h. Cells were then washed with PBS and incubated with Q3G (10 μM) or Me_2SO vehicle (0.05%) for 6 h. Following a rinse in PBS, the cells were subjected to the H_2O_2 insult (500 μM for 15 min) and incubated in growth medium for 6 h. Cells were then washed twice with PBS and harvested by trypsinization. Cells were resuspended in 200 μl of Tris buffer (20 mM, pH 7.4) containing 0.1% Triton X-100 and lysed by sonication on ice. Protein was estimated in the cell lysate using the Bio-Rad reagent. Lipids were extracted using 200 μl of choloroform/methanol (2:1), the solvent was completely evaporated in a SpeedVac (Savant), and the lipids were resuspended in 50 μl of choloroform/methanol (2:1) and spotted onto thin silica plates (LK6D Silica Gel 60A; Whatman) along with the [^{14}C]cholesterol standard (Amersham Biosciences). TLC was performed using cyclohexane/ethyl acetate (50:50), and the plates were developed by autoradiography. The spots corresponding to cholesterol were scrapped, and radioactivity was measured by scintillation counting (Beckman Coulter). The data were expressed as incorporation of [^{14}C]acetate into [^{14}C]cholesterol (cpm/mg of protein).

Inhibition of Cholesterol Synthesis Using Mevastatin—Cells were seeded in a 96-well plate at a density of 1×10^4 cells/100 μl and treated with Q3G (10 μM) for 6 h. Following a rinse in PBS, the cells were subjected to the H_2O_2 insult (500 μM for 15 min). After several washes, cells were incubated with the inhibitor of HMG-CoA reductase, mevastatin (1 μM) (LKT Laboratory) for 18 h. Cell viability was measured using the MTT assay as described. Absorbance was measured at 562 nm using an ELx800$_{uv}$ microplate reader (Bio-tek Instruments). The resultant data were expressed as percentage viability compared with untreated controls.

Inhibition of Cholesterol Synthesis Using OSCi—SH-SY5Y cells were seeded in a 96-well plate at a density of 1×10^4 cells/100 μl and treated with Q3G (10 μM) for 6 h. Following a rinse in PBS, the cells were subjected to the H_2O_2 insult (500 μM for 15 min). After several washes, cells were incubated with OSCi (3 and 30 nM, respectively) for 18 h. OSCi was dissolved in Me_2SO with a final concentration not exceeding 0.05%. Cell viability was measured using the MTT assay as described. Absorbance was measured at 562 nm using an ELx800$_{uv}$ microplate reader (Bio-tek Instruments). The resultant data were expressed as the percentage of viable cells relative to untreated controls.

Isopentenyl Pyrophosphate (IPP) Rescue Studies—SH-SY5Y cells were seeded in a 96-well plate at a density of 1×10^4 cells/100 μl and treated with Q3G (10 μM) for 6 h. Following a rinse in PBS, the cells were subjected to the H_2O_2 insult (500 μM for 15 min). Cells were incubated with mevastatin (1 μM) alone or mevastatin (1 μM) with varying concentrations of IPP triammonium salt solution (25 and 50 μM; Sigma) or IPP vehicle (1% methanol) for 18 h. The MTT assay was performed as described. Absorbance was measured at 562 nm using an ELx800$_{uv}$ microplate reader (Bio-tek Instruments). The resultant data were expressed as the percentage of viable cells compared with untreated controls.

Transfection Studies—To measure the LDLr induction, SH-SY5Y cells were co-transfected with 900 ng of LDLp-588luc and 100 ng of β-galactosidase plasmid using Lipofectamine 2000 reagent (Invitrogen). SH-SY5Y cells were plated at a density of 2×10^5 cells/500 μl and maintained at 37 °C in a 5% CO_2 incubator for 18 h. SH-SY5Y cells were transfected in 250 μl of serum-free medium for 6 h, and then an equal volume of Dulbecco's modified Eagle's medium containing 20% fetal bovine serum was added to the cells. After 24 h, the medium was replaced, and the cells were incubated with 10 μM Q3G or Me_2SO vehicle (0.05%) for 6 h. Following a rinse with PBS, the cells were exposed to 500 μM H_2O_2 for 15 min and placed in the growth medium for 6 h. Cell lysates were prepared using the lysis buffer by a repetitive freeze-thaw method (Promega). Luciferase activity was determined, and normalization was achieved by measuring β-galactosidase activity as per the manufacturer's instructions (Promega). Data were expressed as -fold increase in luciferase activity relative to β-galactosidase activity.

Western Blot Analysis for SREBP-2—SH-SY5Y cells were seeded in a 6-well plate at a density of 5×10^5 cells/ml. The cells were treated with Q3G (10 μM) or Me_2SO vehicle (0.05%) for 6 h. The cells were then rinsed with PBS and subjected to H_2O_2 insult (500 μM for 15 min). Following a rinse with PBS, the cells were allowed to recover in growth medium for 6 h. Western blot analysis for SREBP-2 was also performed using HEK293 cells (supplemental Fig. 5, *B* and *C*). HEK293 cells were seeded in a 6-well plate at a density of 2×10^5 cells/ml. The cells were treated with 0.1 μM Q3G or Me_2SO vehicle (0.0005%) for 6 h. The cells were then rinsed with PBS and subjected to H_2O_2 insult (500 μM for 3 h). Following a rinse with PBS, the cells were allowed to recover in growth medium for 6 h. Whole cell protein extracts were prepared from SH-SY5Y and HEK293 cells using radioimmune precipitation buffer (1% Triton X-100, 0.04% SDS, 0.037 M NaCl, 0.05 M Tris-HCl base, and 0.32 M deoxycholic acid, pH 8.0) containing a protease inhibitor mixture (Roche Applied Science). Protein concentration in cell lysates was estimated using a Bio-Rad reagent. Briefly, 20 μg of protein was resolved on a 12.5% SDS-PAGE and transferred to polyvinylidene difluoride transfer membrane (Millipore Corp.). The membranes were blocked (5% nonfat milk powder in TBS and 0.1% Tween 20) at room temperature for 1 h and incubated with a SREBP-2 primary antibody (BD Biosciences) at a dilution of 1:1000 at 4 °C overnight. Following several washes, the membranes were incubated with peroxidase-conjugated anti-mouse secondary antibody (Vector Laboratories) at a 1:2500 dilution at room temperature for 1 h. Following several washes, immunoreactivity was visualized using the ECL chemiluminescence kit according to the manufacturer's

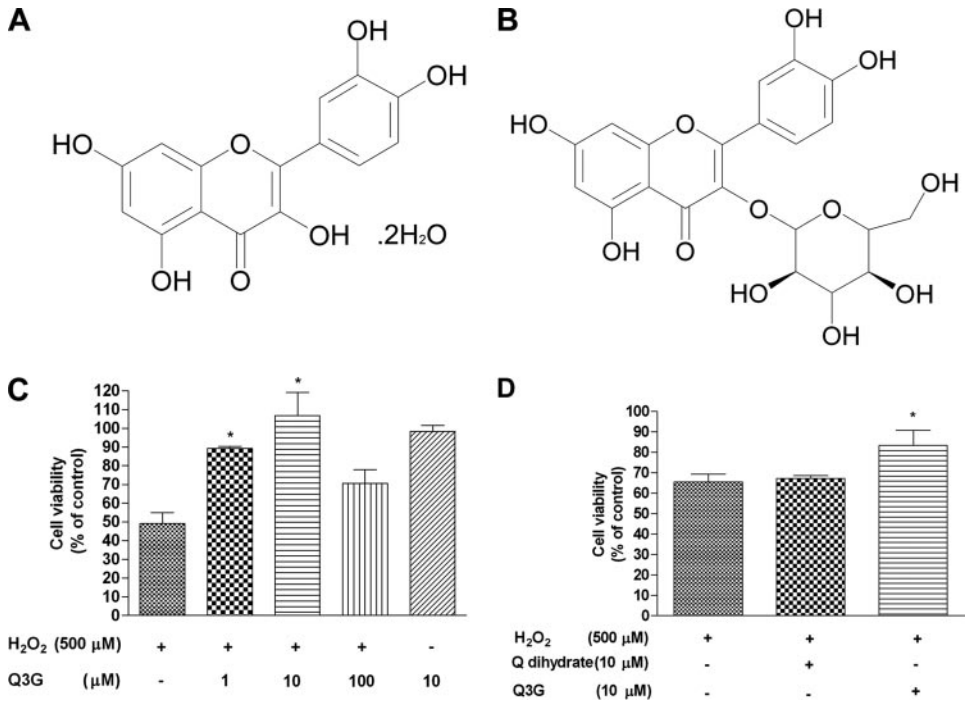

FIGURE 1. **Q3G protects SH-SY5Y cells against cell death induced by oxidative stress.** *A*, structure of Q dihydrate. *B*, structure of Q3G. *C*, MTT assay depicting the dose-response curve of SH-SY5Y cells pretreated with various concentrations of Q3G for 18 h prior to oxidative insult. The data are represented as percentage of cell viability relative to untreated cells. Each *bar* represents the mean ± S.E. of 16 determinations from two independent experiments. *, $p < 0.05$ *versus* H_2O_2-treated cells. *D*, SH-SY5Y cells were pretreated with Q dihydrate or Q3G for 18 h prior to the oxidative insult, and MTT assay was performed as described previously. The data are represented as percentage of cell viability relative to untreated cells. Each *bar* represents the mean ± S.E. from 16 determinations from two independent experiments. *, $p < 0.05$ *versus* H_2O_2-treated cells.

instructions (Amersham Biosciences). The blots were exposed to x-ray film (Eastman Kodak Co.) for 24 h and developed using a Kodak developer. The data were expressed as -fold induction of cleaved active SREBP-2 (65 kDa) to total SREBP-2 (uncleaved precursor form of SREBP-2 (110 kDa) + cleaved active form of SREBP-2 (65 kDa)) normalized to β-actin levels.

siRNA Studies—Transfection studies in SH-SY5Y cells were carried out using siRNA-targeting SREBP-2. siRNAs were purchased from Ambion. Silencer predesigned siRNA oligonucleotides (sense, 5′-GGCUUUGAAGACGAAGCUAtt-3′; antisense, 5′-UAGCUUCGUCUUCAAAGCCtg-3′) targeting SREBP-2 were used. As a negative control, siRNA containing 19-bp nontargeting sequences with 3′ dT overhangs was used to rule out nonspecific effects on gene expression. To standardize the conditions for transient transfection, we seeded cells in 24-well plates at a density of 5×10^4 cells/500 μl. Transfection was carried out using 3 μl of Lullaby transfection reagent (OZ Biosciences) and 15 pmol of siRNA (final concentration was 30 nM) for 3 h as per the manufacturer's instructions (OZ Biosciences). The medium was replaced, and cells were incubated at 37 °C in a 5% CO_2 incubator for 24 h. Total RNA was extracted using the RNeasy kit (Qiagen), and siRNA knockdown of SREBP-2 was confirmed by one-step RT-PCR (Clontech) using 100 ng of total RNA and primers 5′-CCCTTCAGTGCAACGGTCATTCAC-3′ and 5′-GATGCTCAGTGGCACTGACTCTTC-3′ as sense and antisense primers, respectively (33) (product size, 401 bp) as per the manufacturer's instructions. The RT-PCR product was loaded on a 2% agarose gel and visualized by ethidium bromide staining. As an internal control, we used 18S RNA to normalize the loading. Similarly, we carried out RT-PCR using SREBP-1 primers 5′-CTGCTGACCGACATCGAAGAC-3′ and 5′-GATGCTCAGTGGCACTGACTC-3′ as sense and antisense primers, respectively (33) (product size, 321 bp) as per the manufacturer's instructions.

The cells were seeded in a 96-well plate at a density of 1×10^4 cells/100 μl. siRNA studies were performed using SREBP-2 siRNA and the silencer negative control siRNA, as described previously. After 24 h post-transfection, the cells were incubated with Q3G (10 μM) or Me_2SO vehicle (0.05%) for 6 h. Following a rinse with PBS, the cells were exposed to 500 μM H_2O_2 for 15 min and placed in growth medium for 18 h. The MTT assay was then performed as described. The resultant data were expressed as the percentage of viable cells compared with untreated controls.

Statistical Analysis—Data analysis was performed using Student's *t* test, one-way analysis of variance, and Tukey's *post hoc* test using GraphPad Prism version 3. An α value of <0.05 was considered to be significant.

RESULTS

Q3G but Not Quercetin Dihydrate Protected SH-SY5Y, HEK293, and MCF-7 Cells against Oxidative Damage—Q3G differs from the parent compound Q dihydrate (Fig. 1*A*) in having a glucoside moiety attached to carbon atom -3 on the C-ring (Fig. 1*B*). In the present study, we investigated the cytoprotective effect of Q3G and Q dihydrate against H_2O_2-induced oxidative stress in various cell lines. First, we determined the dose and time of exposure to H_2O_2 to reduce cell viability by 50%. Treatment of SH-SY5Y cells with 500 μM of H_2O_2 for 15 min resulted in a 40% decrease in cell viability relative to untreated cells (supplemental Fig. 1*A*). The dose- and time-response curves for HEK293 and MCF-7 cells exposed to H_2O_2 demonstrated that these cells were completely resistant to this insult at a concentration and exposure time that caused a 50% loss of cellular viability in SH-SY5Y cells. Exposure to a concentration of 500 μM of H_2O_2 for 3 h was required to kill 50% of HEK293 cells (supplemental Fig. 1*B*), whereas 800 μM H_2O_2 for 24 h produced only a 20% loss in cell viability in MCF-7 cells (supplemental Fig. 1*C*).

Pretreatment with Q3G increased viability by ~40% (1 μM) and 55% (10 μM) relative to cells treated with H_2O_2 alone (Fig.

1*C*). Q3G showed a biphasic response as a concentration of 100 μM did not afford any protection against the H_2O_2 insult (Fig. 1*C*). Treatment with 10 μM Q3G alone did not alter cell viability relative to control cells that were not treated with the flavonoid or exposed to oxidative stress (Fig. 1*C*). These results indicate that 10 μM Q3G provided maximal protection from the loss of cell viability produced by the H_2O_2 insult, and at this concentration Q3G was not cytotoxic; nor did it alter the rate of cell division (Fig. 1*C*). Pretreatment with 10 μM Q dihydrate did not protect cells against H_2O_2 insult. This implies that at the concentrations tested in this model, Q3G is an effective cytoprotectant, whereas Q dihydrate is not (Fig. 1*D*).

HEK293 cells pretreated with different concentrations of Q3G (0.01–10 μM) for 6 h showed an inverted U-shaped reversal of H_2O_2-induced cell death with a peak reversal of hydrogen peroxide-induced death of 50% generated by the 0.1 μM Q3G, whereas 10 μM Q3G failed to protect against H_2O_2-induced oxidative insult (supplemental Fig. 1*D*). The Me_2SO vehicle did not exert any protective effect against H_2O_2-induced oxidative insult (supplemental Fig. 1*D*). Treatment with 10 μM Q3G alone did not alter cell viability relative to untreated cells (supplemental Fig. 1*D*). In contrast, Q dihydrate was not effective against H_2O_2-induced oxidative insult at any of the concentrations tested (data not shown). Similarly, pretreatment of MCF-7 cells with varying concentrations of Q3G for 6 h produced an inverted U shaped protection against H_2O_2-induced oxidative death, with a concentration of 0.1 μM Q3G producing a 50% increase in cell survival (supplemental Fig. 1*E*). As was observed in HEK293 cells, Q dihydrate was not effective against the injurious effects of H_2O_2 at any of the concentrations tested (data not shown). We therefore demonstrate that Q3G protected against oxidative stress in SH-SY5Y, HEK 293, and MCF-7 cells, whereas Q dihydrate was ineffective.

Q3G Protected SH-SY5Y Cells against H_2O_2-induced Cell Death—Having established that Q3G (10 μM) exerted a cytoprotective effect in SH-SY5Y cells against oxidative stress, we explored whether protection was mediated by reducing apoptotic and/or necrotic cell death. SH-SY5Y cells exposed to 500 μM H_2O_2 for 15 min showed a 2-fold increase in nucleosomal enrichment factor compared with untreated cells (Fig. 2*A*). This was comparable with the magnitude of nucleosomal enrichment produced by the positive control. Pretreatment of SH-SY5Y cells with Q3G (10 μM) or a positive control, tBHQ (5 μM) resulted in a significant reduction in cell death compared with cells treated with either a hypertonic solution or H_2O_2 (Fig. 2*A*).

Next, we determined the effect of the H_2O_2 insult on the membrane integrity of SH-SY5Y cells by examining extracellular levels of the intracellular enzyme LDH. The release of LDH from the cell membrane is a marker for necrotic cell death. We found that H_2O_2 caused an increase in LDH release compared with untreated control (Fig. 2*B*). Pretreatment with Q3G reduced the increase in LDH release induced by H_2O_2 by ~66% relative to those cells exposed to H_2O_2 alone (Fig. 2*B*). Since cholesterol is a major constituent of the plasma membrane and contributes to membrane integrity, we used an inhibitor of cholesterol synthesis (mevastatin, HMG-CoA reductase inhibitor) to assess the protective effects of Q3G pretreatment in

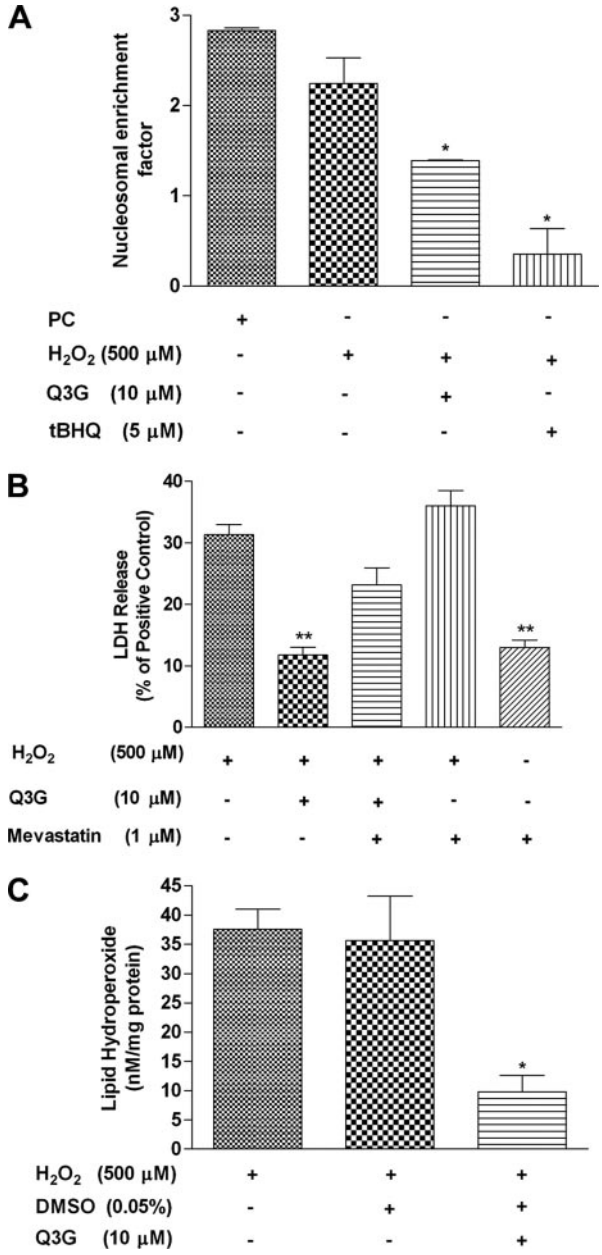

FIGURE 2. **Cellular and metabolic effects of Q3G-mediated cytoprotection against oxidative stress.** *A*, cell death ELISA (*CDE*). SH-SY5Y cells were pretreated with Q3G (10 μM) or tBHQ (5 μM) for 18 h prior to the oxidative insult. CDE was performed as described under "Experimental Procedures." Data are expressed as nucleosomal enrichment factor. Each *bar* represents the mean ± S.E. of four determinations from two independent experiments. *PC*, positive control. *, $p < 0.05$ *versus* H_2O_2-treated cells. *B*, LDH assay. SH-SY5Y cells were pretreated with 10 μM Q3G or 0.05% Me_2SO for 6 h prior to the oxidative insult. The medium was replaced, and cells were incubated with 1 μM mevastatin for 18 h. A CytoTox96 nonradioactive cytotoxicity assay was performed to assay for LDH release as described under "Experimental Procedures." Data are expressed as percentage of LDH release compared with the positive control. Each *bar* represents the mean ± S.E. of 24 determinations from three independent experiments **, $p < 0.01$ relative to H_2O_2-treated cells. *C*, lipid peroxidation assay. SH-SY5Y cells were pretreated with 10 μM Q3G or 0.05% Me_2SO (*DMSO*) for 6 h prior to the oxidative insult. Lipid hydroperoxides were measured in the Q3G or Me_2SO-treated samples. Data were extrapolated from the standard curve as described under "Experimental Procedures." The data are expressed as nM lipid hydroperoxides/mg of protein. Each *bar* represents the mean ± S.E. of six determinations from three independent experiments. *, $p < 0.05$ relative to H_2O_2-treated cells.

SH-SY5Y cells exposed to oxidative damage. The addition of mevastatin partially reversed the protective effects of Q3G pretreatment, and mevastatin alone did not increase LDH release (Fig. 2*B*).

We used TUNEL staining to identify cells injured by oxidative stress (supplemental Fig. 2*A*). Like the positive control, cells exposed to H_2O_2 were TUNEL-positive. Pretreatment with Q3G prior to the oxidative insult significantly decreased the number of TUNEL-positive cells. To further evaluate the mechanism of cell death induced by H_2O_2, Western blot analysis was carried out using an antibody that detects caspase-3-cleaved spectrin (36). In SH-SY5Y cells treated with H_2O_2, higher levels of caspase-3-cleaved spectrin were detected compared with untreated cells (data not shown). Pretreatment of SH-SY5Y cells with Q3G or Me_2SO did not reduce the levels of H_2O_2-induced caspase-3 activation (data not shown). Pretreatment with Q3G alone did not induce apoptosis (data not shown).

In SH-SY5Y cells, H_2O_2 activated both necrotic as well as apoptotic pathways. Based on a failure to reduce caspase-3 activation, we conclude that Q3G protected SH-SY5Y cells against necrotic rather than apoptotic cell death.

Q3G Pretreatment Reduces Intracellular ROS—The ability of quercetin to scavenge free radicals is well documented; however, little is known about the free radical scavenging abilities of Q3G. SH-SY5Y cells treated with H_2O_2 and horseradish peroxidase showed a 2.5-fold increase in ROS activity compared with untreated control cells (supplemental Fig. 2*B*). Pretreatment with Q3G (5 μM) produced a nearly complete reversal of intracellular ROS to those observed in cells not exposed to oxidative stress (supplemental Fig. 2*B*). Pretreatment with 5 μM tBHQ produced a reduction in ROS levels comparable with 10 μM Q3G; however, 10 μM tBHQ did not reduce ROS levels. Vehicle-treated samples displayed a small reduction in intracellular ROS levels. However, this reduction was not statistically significant (supplemental Fig. 2*B*). These results indicate that Q3G protected SH-SY5Y cells from the injurious effects of oxidative stress.

Lipid Peroxidation Assay—In SH-SY5Y cells subjected to H_2O_2-induced oxidative stress, we detected 40 nM lipid hydroperoxides/mg of protein. Pretreatment of SH-SY5Y cells with Q3G led to a significant decrease in lipid peroxidation by 4-fold compared with H_2O_2-treated cells (Fig. 2*C*). In cells pretreated with Me_2SO vehicle, there was an increase in lipid hydroperoxides comparable with H_2O_2-treated cells (Fig. 2*C*). Since the assay is very sensitive and measures the initial products of lipid peroxidation rather than the secondary breakdown products, the estimation of lipid peroxidation is more reliable, and it is not overestimated as compared with other methods of detection (*i.e.* thiobarbituric acid reactive substances assay). We conclude from these studies that Q3G pretreatment is effective in reducing H_2O_2-induced lipid peroxidation.

Gene Profiling Using cDNA Microarray Implicated Elevated Cholesterol Biosynthesis in Q3G-mediated Cytoprotection—Treatment of SH-SY5Y cells with Q3G alone did not alter gene expression in SH-SH5Y cells compared with cells that were treated with Me_2SO vehicle. Significance Analysis of Microarray (SAM) revealed one significantly up-regulated gene at a false discovery rate of 0% and a Δ value of 0.381 (supplemental Fig. 3*A*). Pretreatment of cells with Q3G followed by oxidative stress resulted in altered gene expression compared with Me_2SO-treated cells. SAM analysis showed that at a Δ value of 0.266, there were 28 significantly altered genes (25 up-regulated and three down-regulated genes) with a false discovery rate of 7.31% (supplemental Fig. 3*B*). Putative functional linkages between the genes modulated by Q3G under oxidative stress revealed that 16 of 25 (64%) of these genes are involved in the cholesterol and lipid pathway (supplemental Fig. 3*C*).

Confirmation of cDNA Microarray Findings by qRT-PCR—The changes in the expression of SCD1, HMG-CoA reductase, and sestrin 1 as determined by cDNA microarray were all confirmed by qRT-PCR (supplemental Fig. 4, *A–C*, respectively). In SH-SY5Y cells subjected to the H_2O_2 insult, both SCD1 and HMG-CoA reductase transcripts were unchanged compared with untreated cells (supplemental Fig. 4, *D* and *E*, respectively).

Q3G Pretreatment Results in Elevated Cholesterol Levels after Oxidative Stress—The -fold increases in expression of genes that were up-regulated by Q3G under oxidative stress as determined by cDNA microarray (*black*) and qRT-PCR (*bracketed*) in the cholesterol biosynthetic pathway are shown in Fig. 3*A*. Since many of the up-regulated genes are involved in cholesterol biosynthesis, cholesterol levels were determined. Cells treated with vehicle and then exposed to oxidative stress did not show an increase in cholesterol levels over cells exposed to oxidative stress alone (Fig. 3*B*). By contrast, cells pretreated with Q3G and then exposed to oxidative stress showed a significant increase in cholesterol levels of ~35%, compared with vehicle-treated cells exposed to the oxidative insult (Fig. 3*B*).

Q3G Pretreatment Enhanced de Novo Cholesterol Synthesis in SH-SY5Y Cells Subjected to Oxidative Stress—SH-SY5Y cells pretreated with Q3G showed a 2-fold increase in conversion of [^{14}C]acetate into [^{14}C]cholesterol under oxidative stress compared with Me_2SO-treated cells (Fig. 3*C*). Cells treated with H_2O_2 alone did not show an increase in cholesterol biosynthesis compared with untreated cells. Moreover, basal cholesterol biosynthesis was not altered by either Q3G or Me_2SO alone (Fig. 3*C*).

These results indicate that Q3G pretreatment increased total cellular cholesterol and enhanced *de novo* cholesterol synthesis in SH-SY5Y cells subjected to oxidative stress.

Mevastatin Reduced the Cytoprotective Effects of Q3G—Mevastatin, an inhibitor of HMG-CoA reductase, was used to inhibit cholesterol synthesis in SH-SY5Y cells in order to determine whether cholesterol biosynthesis mediated Q3G-induced cytoprotection against oxidative stress. Pretreatment with Q3G reversed the loss of cell viability produced by oxidative stress by about 25% (Fig. 4*A*). This protective effect of Q3G was reversed by the addition of mevastatin after the H_2O_2 insult (Fig. 4*A*). By contrast, mevastatin (1 μM) did not alter the loss of cell viability produced by the H_2O_2 insult; nor did it alter cell viability when added on its own compared with untreated cells, suggesting that the concentration of mevastatin used was noncytotoxic (Fig. 4*A*).

Effect of OSCi on Cytoprotective Effects of Q3G—The 2,3-oxidosqualene:lanosterol cyclase inhibitor, OSCi, was used to

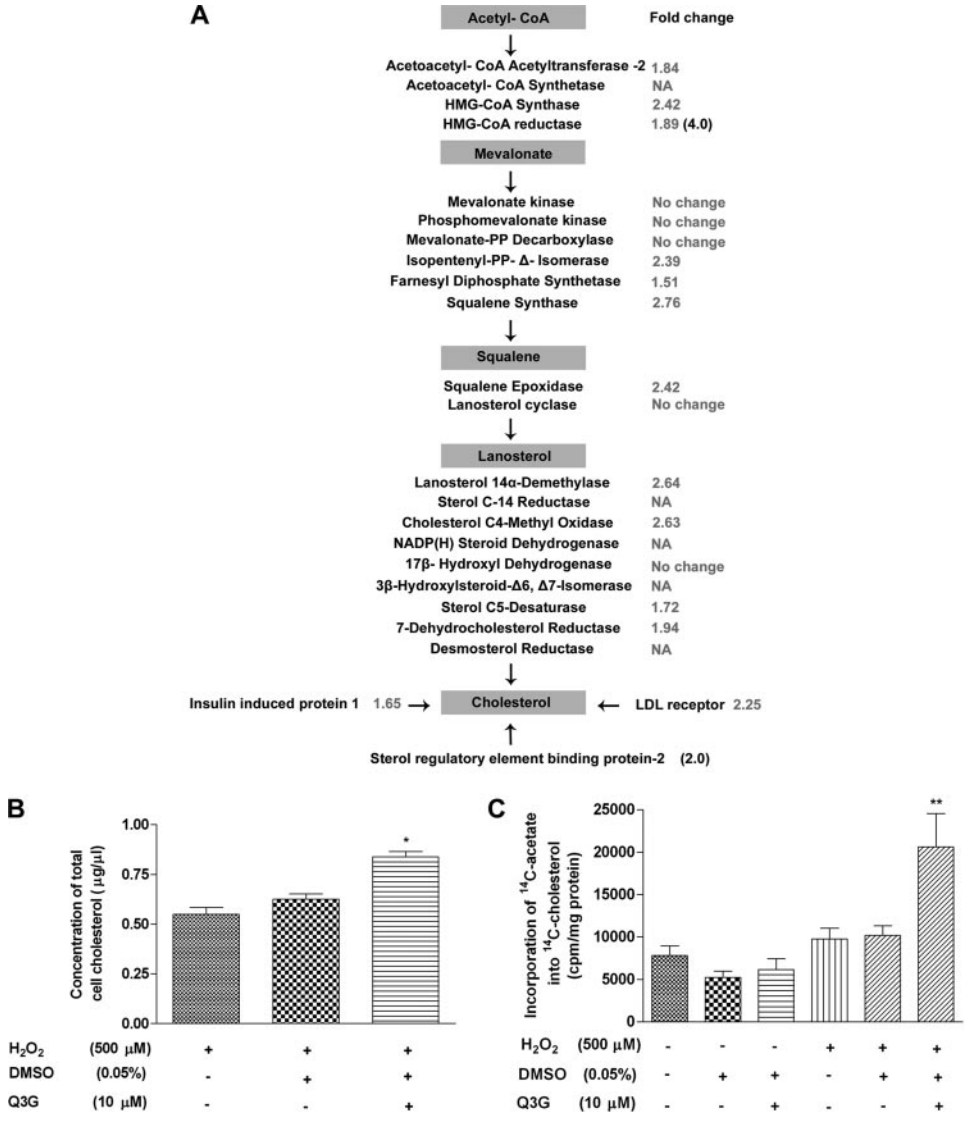

FIGURE 3. **Q3G induces cholesterol synthesis in SH-SY5Y cells under oxidative stress.** *A*, SREBP-2-mediated cholesterol biosynthetic pathway in mammalian cells. The key intermediary steps in the *de novo* cholesterol pathway from acetyl-CoA are shown. The -fold changes in the genes up-regulated by Q3G under oxidative stress as identified by cDNA microarray (SAMF human 14K) are shown in *black*, whereas elevations measured by qRT-PCR are *bracketed*. *NA*, not applicable; these genes are not represented on the SAMF human 14K chip. *B*, determination of total cell cholesterol. SH-SY5Y cells pretreated with 10 μM Q3G or 0.05% Me_2SO (*DMSO*) vehicle for 6 h was subjected to the oxidative insult. Cholesterol and cholesterol esters were measured in the Q3G- or Me_2SO-treated samples. Data were extrapolated from the standard curve as described under "Experimental Procedures." Data are expressed as the concentration of total cell cholesterol ($\mu g/\mu l$) in each sample. Each *bar* represents the mean ± S.E. of six determinations from three independent experiments. *, $p < 0.05$; H_2O_2-treated cells. *C*, *de novo* cholesterol synthesis. SH-SY5Y cells were incubated with 1 μCi of [^{14}C]acetate for 24 h. SH-SY5Y cells pretreated with 10 μM Q3G or 0.05% Me_2SO vehicle for 6 h were subjected to the oxidative insult. After 18 h, lipids were extracted, cholesterol was separated using TLC, and scintillation counting was performed as described under "Experimental Procedures." Data are expressed as incorporation of [^{14}C]acetate into [^{14}C]cholesterol (cpm/mg of protein). Each *bar* represents the mean ± S.E. of six determinations from two independent experiments performed. **, $p < 0.01$ relative to H_2O_2-treated cells.

determine the effects of selective inhibition of cholesterol synthesis on Q3G-mediated cytoprotection against oxidative stress. Pretreatment with Q3G improved cell viability by about 12% under oxidative stress (Fig. 4*B*). This protective effect of Q3G was reversed by the addition of 30 nM OSCi after the H_2O_2 insult (Fig. 4*B*). OSCi at a concentration of 3 nM was not effective in reversing the cytoprotective effect of Q3G against oxidative stress induced by H_2O_2. OSCi at a concentration of 30 nM did not alter cell viability after the H_2O_2 insult. Treatment of cells with OSCi alone did not alter cell viability compared with untreated cells, suggesting that the concentration of OSCi used in the study was noncytotoxic. These observations indicate that selective inhibition of cholesterol synthesis by OSCi abrogates the protective effect of Q3G.

Inhibition of Cholesterol and Isoprenoid Pathway Induced by Mevastatin Is Rescued by IPP Treatment—Pretreatment of SH-SY5Y cells with mevastatin (1 μM) inhibited the protective effect of Q3G under oxidative stress. This was rescued by the addition of 50 μM of IPP to cells (Fig. 4*C*). A concentration of 25 μM IPP was not effective in rescuing the effect of mevastatin inhibition on Q3G-mediated protection under oxidative stress (Fig. 4*C*). A concentration of IPP (50 μM) on its own was noncytotoxic. Also, the vehicle used to dissolve IPP did not alter cell viability (Fig. 4*C*). We therefore conclude that the isoprenoid pathway is not involved in Q3G-mediated cytoprotection.

Increased Levels of SREBP-2 mRNA in Q3G-pretreated SH-SY5Y Cells Subjected to Oxidative Stress—Quantitative RT-PCR revealed a 2-fold increase in the expression of SREBP-2 mRNA only in cells pretreated with Q3G and subjected to oxidative stress (Fig. 5*A*). In comparison with Q3G, pretreatment of SH-SY5Y cells with Q dihydrate did not alter the mRNA levels of SREBP-2 (Fig. 5*B*).The expression of SREBP-2 mRNA was unaffected by oxidative stress alone (data not shown). These results are consistent with our cDNA microarray results, suggesting that Q3G, but not Q dihydrate, increased levels of transcripts encoding SREBP-2 in cells under oxidative stress.

In HEK293 cells pretreated with Q3G, there was also a slight but significant increase in the SREBP-2 transcript under oxidative stress (supplemental Fig. 5*A*). In MCF-7 cells, preliminary RT-PCR data indicated no change in the SREBP-2 transcript in either treated or untreated groups (data not shown).

Enhanced Expression of LDLr in SH-SY5Y Cells Pretreated with Q3G and Subjected to Oxidative Stress—Transient transfection of SH-SY5Y cells with LDL plasmid was used to assess

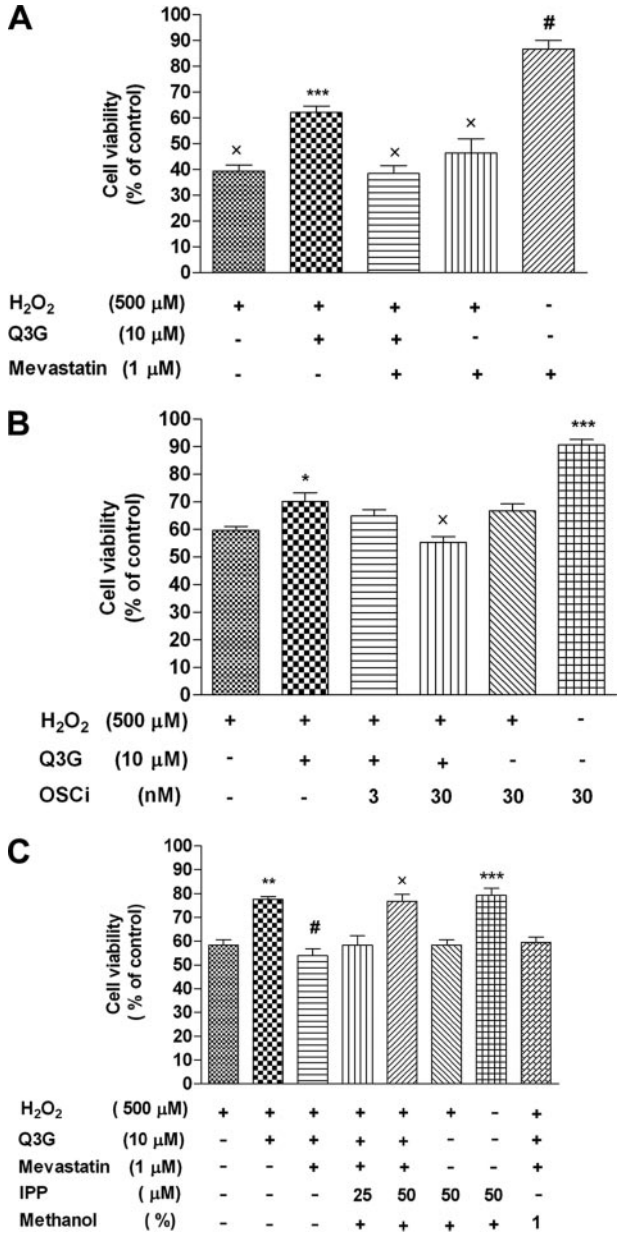

FIGURE 4. **Effect of cholesterol synthesis inhibitors on Q3G mediated cytoprotection.** *A*, SH-SY5Y cells pretreated with 10 μM Q3G or 0.05% Me_2SO vehicle for 6 h was subjected to the oxidative insult. Following the insult, Q3G-pretreated cells were incubated with 1 μM mevastatin for 18 h. Cell viability was assessed by MTT assay as described under "Experimental Procedures." Each *bar* represents the mean ± S.E. of 24 determinations from three independent experiments. ***, $p < 0.001$ relative to all groups including H_2O_2-treated cells. ×, ***, $p < 0.001$ relative to all groups including the untreated cells. #, ***, $p < 0.001$ relative to all other groups. *B*, SH-SY5Y cells pretreated with 10 μM Q3G or 0.05% Me_2SO vehicle for 6 h were subjected to the oxidative insult. Following the insult, Q3G-pretreated cells were incubated with OSCi (3 and 30 nM, respectively) for 18 h. MTT assay was then performed as described under "Experimental Procedures." Data are represented as percentage of cell viability relative to the untreated cells. Each *bar* represents the mean ± S.E. of 24 determinations from three independent experiments. *, $p < 0.05$ relative to H_2O_2-treated cells except for the Q3G + H_2O_2 + OSCi (3 nM) group and H_2O_2 + OSCi (30 nM) group. ×, ***, $p < 0.001$ relative to Q3G + H_2O_2 group and OSCi (30 nM) only group. ×, *, $p < 0.05$ relative to the Q3G + H_2O_2 + OSCi (3 nM) group and H_2O_2 + OSCi (30 nM) group except for the H_2O_2 group. ***, $p < 0.001$ relative to all groups. *C*, SH-SY5Y cells pretreated with 10 μM Q3G or 0.05% Me_2SO vehicle for 6 h was subjected to the oxidative insult. Following the insult, Q3G-pretreated cells were incubated with 1 μM mevastatin and isopentenyl pyrophosphate (25 and 50 μM) for 18 h. Cell viability was assessed by MTT assay as described under "Experimental Procedures." Each *bar* represents the mean ± S.E. of 24 determinations from three independent experiments. **, $p < 0.01$ relative to all other groups, including H_2O_2-treated cells, except for the Q3G + H_2O_2 + mevastatin + IPP (50 μM) group and the IPP (50 μM) only group. #, ***, $p < 0.001$ relative to all other groups except for the Q3G + H_2O_2 + mevastatin + IPP (25 μM) group, H_2O_2 + IPP (50 μM) group, and Q3G + H_2O_2 + mevastatin + vehicle (1% methanol) group. ×, ***, $p < 0.001$ relative to the Q3G + H_2O_2 + mevastatin group. ×, **, $p < 0.01$ relative to all other groups except for the Q3G + H_2O_2 group and IPP (50 μM) only group. ***, $p < 0.001$ relative to all other groups except for the Q3G + H_2O_2 group and IPP (50 μM) only group.

whether Q3G up-regulated the expression of LDLr, a SREBP-2-regulated gene under oxidative stress. In SH-SY5Y cells treated with Me_2SO or Q3G and not subjected to oxidative insult, relative luciferase levels were unchanged, indicating no induction of the LDL receptor (Fig. 5*C*). However, SH-SY5Y cells pretreated with Q3G and subjected to oxidative stress showed a significant increase in relative luciferase levels, indicating induction of the LDLr compared with DMSO + H_2O_2-treated or H_2O_2-treated controls (Fig. 5*C*).

Q3G Induces the Processing of Transcriptionally Active SREBP-2 from Its Precursor in SH-SY5Y Cells under Oxidative Stress—We compared levels of the transcriptionally inactive precursor form of SREBP-2 (110 kDa) and the transcriptionally active cleaved form of SREBP-2 (65 kDa) in SH-SY5Y cells by Western blotting. In untreated or Me_2SO- or Q3G-treated cells, the levels of uncleaved transcriptionally inactive SREBP-2 (110 kDa) appeared higher than the levels of cleaved transcriptionally active SREBP-2 (65 kDa) (Fig. 6*A*). In cells pretreated with Q3G and exposed to oxidative stress, levels of active SREBP-2 (65 kDa) relative to uncleaved transcriptionally inactive SREBP-2 (110 kDa) appeared higher than that observed in cells exposed to only oxidative stress (H_2O_2) or vehicle (0.05% Me_2SO) + H_2O_2 (Fig. 6*B*). This suggests that the combination of Q3G pretreatment followed by oxidative stress led to an increase in the cleaved form of SREBP-2. Densitometric scans of the Western blots revealed over a 2-fold increase in transcriptionally active SREBP-2 compared with total SREBP-2 in cells receiving Q3G pretreatment and subjected to oxidative stress (Fig. 6*C*).

When compared with SH-SY5Y cells, Western blot analysis of SREBP-2 derived from HEK293 whole cell lysates showed a different pattern. In untreated or Me_2SO- or Q3G (0.1 μM)-treated cells, the levels of uncleaved or transcriptionally inactive SREBP-2 precursor (130 kDa) were low compared with the cleaved or transcriptionally active form of SREBP-2 (65 kDa) (supplemental Fig. 5*B*). Cells pretreated with either Q3G or Me_2SO prior to the H_2O_2 insult also failed to demonstrate an activation of SREBP-2 (supplemental Fig. 5*C*). These observations indicate that SREBP-2 pathway is activated only in SH-SY5Y cells pretreated with Q3G and subjected to oxidative stress.

siRNA-mediated Knockdown of SREBP-2 Abolishes the Protective Effect of Q3G—In order to specifically silence the SREBP-2 gene, SH-SY5Y cells were transfected with siRNA targeting SREBP-2 mRNA. RT-PCR demonstrated that there was a concentration-dependent suppression of SREBP-2 mRNA by the SREBP-2 siRNA compared with cells transfected with the negative control siRNA. No effect of siRNA was observed on 18S mRNA expression that served as an internal control (Fig.

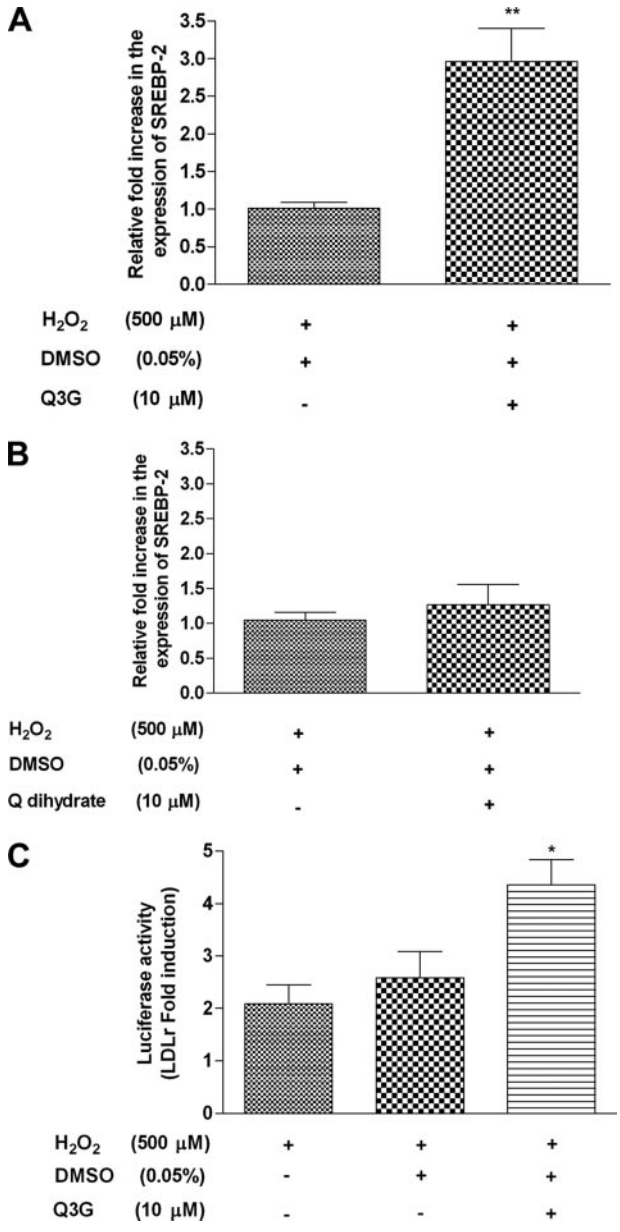

FIGURE 5. **Q3G increases SREBP-2 mRNA levels and LDLr expression under oxidative stress.** *A*, SH-SY5Y cells were pretreated with 10 μM Q3G or 0.05% Me_2SO (*DMSO*) for 6 h prior to the oxidative insult. Total RNA was extracted, and qRT-PCR was performed using SREBP-2 primers. Relative quantification of SREBP-2 is shown. Data are expressed as the relative -fold increase in the gene expression after normalization to an internal control, GAPDH. Each *bar* represents the mean ± S.E. of four determinations from two independent experiments. **, $p < 0.01$ *versus* Me_2SO-treated cells. *B*, SH-SY5Y cells were pretreated with 10 μM Q dihydrate or 0.05% Me_2SO for 6 h prior to the oxidative insult. Total RNA was extracted, and qRT-PCR was performed using SREBP-2 primers. Relative quantification of SREBP-2 is shown. Data are expressed as the relative -fold increase in the gene expression after normalization to an internal control, GAPDH. Each *bar* represents the mean ± S.E. of four determinations from two independent experiments. *C*, SH-SY5Y cells were transfected with LDLp-588luc and β-galactosidase plasmid for 24 h and pretreated with 0.05% Me_2SO or 10 μM Q3G for 6 h prior to H_2O_2 exposure. Cell lysates were prepared, and luciferase activity was detected as described under "Experimental Procedures." Data are expressed as -fold increase in luciferase activity relative to β-galactosidase activity. Each *bar* represents the mean ± S.E. of six determinations from three independent experiments. *, $p <$ 0.05 relative to H_2O_2-treated cells.

7*A*). At a concentration of 30 nM, there was a complete knockdown of SREBP-2 mRNA relative to the control siRNA 24 h post-transfection. Therefore, 30 nM siRNA was used for all further studies. siRNA-mediated knockdown of SREBP-2 did not suppress the expression of SREBP-1 mRNA. No effect of siRNA was observed on 18S mRNA expression that served as an internal control (Fig. 7*B*).

To assess the effect of SREBP-2 knockdown on Q3G-mediated cytoprotection against oxidative stress, we carried out a MTT assay 48 h post-transfection. The specific knockdown of SREBP-2 led to a 2-fold decrease in cell viability induced by Q3G pretreatment under oxidative stress (Fig. 7*C*). By contrast, the negative control siRNA had no effect on Q3G-mediated protection against oxidative stress (Fig. 7*C*). The concentration of siRNA targeting SREBP-2 (30 nM) or negative control siRNA (30 nM) did not affect cell viability. Moreover, there was no difference in the loss of cell viability upon H_2O_2 insult in transfected *versus* nontransfected cells (Fig. 7*C*). We therefore conclude that inhibition of SREBP-2 expression by siRNA blocks Q3G-mediated cytoprotection in SH-SY5Y cells subjected to oxidative stress.

DISCUSSION

A major finding of the present study was that the flavonoid Q3G protected SH-SY5Y cells from injurious concentrations of H_2O_2 by elevating cellular cholesterol levels through activation of SREBP-2. This novel mechanism occurred only when the cells were pre-exposed to Q3G prior to the H_2O_2 insult, suggesting that transcriptional events where responsible for cytoprotection. This transcriptional response consisted of increased expression of genes responsible for cholesterol biosynthesis that served to increase plasma membrane integrity by limiting lipid peroxidation. In our hands, pretreatment with Q dihydrate did not protect SH-SY5Y cells subjected to oxidative damage. It is therefore not surprising that Q dihydrate failed to activate SREBP-2. Q3G protected HEK 293 and MCF-7 cells from oxidative injury by a mechanism that did not involve either the SREBP-2 signaling or the well known antioxidant-responsive element-Nrf2 antioxidant pathways.

The antioxidant activity of flavonoids has been implicated in the ability of these compounds to prevent ROS-induced cell death (37). Quercetin has been reported to directly scavenge free radicals and chelate metal ions, enabling this compound to reduce single strand DNA breaks, lipid peroxidation, and protein damage (38, 39). The structural basis for the antioxidant activity of Q3G in SH-SY5Y cells may be attributed to chemical features it shares with quercetin, such as the presence of 3′,4′-dihydroxycatechol in the B ring, the inclusion of 2,3-unsaturation in the C-ring, and oxo function in the C-4 position of the C-ring (40, 41). By contrast, the antioxidant activity of quercetin was unaffected by 3-glycosylation in the C-ring, whereas glucosylation at the 4′-position of quercetin abolished both its antioxidant activity and inhibition of lipid peroxidation, further supporting our observations (42). The major chemical difference between Q3G and Q dihydrate used in the present study is the presence of the glucoside group attached to the C ring of Q3G that is absent from Q dihydrate. This may result in a better uptake of Q3G into cells. For example, it is well known that the intestinal sodium-dependent glucose transporter (SGLT1) is involved in Q3G uptake across the brush border membrane of

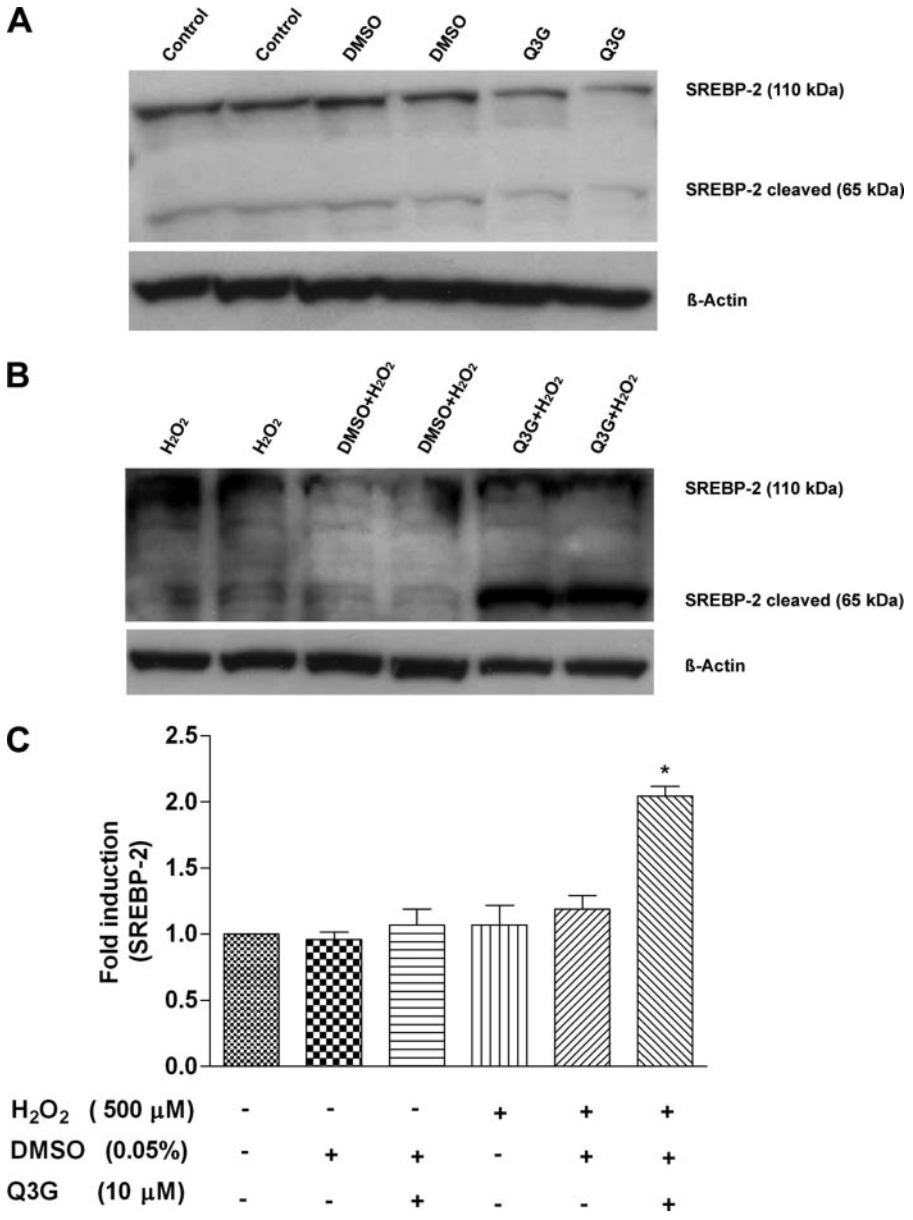

FIGURE 6. **Q3G increases the levels of transcriptionally active SREBP-2 (65 kDa) under oxidative stress.** *A*, Western blot analysis of SREBP-2 protein extracts from untreated cells (*lanes 1* and *2*) or cells pretreated with 0.05% Me_2SO (*DMSO*) (*lanes 3* and *4*) or 10 μM Q3G (lanes *5* and *6*) for 6 h were prepared, as described under "Experimental Procedures." Both uncleaved (110 kDa) and cleaved (65 kDa) forms of SREBP-2 were visualized using an antibody that selectively recognizes SREBP-2. *B*, protein extracts were prepared from SH-SY5Y cells subjected to H_2O_2 insult (*lanes 1* and *2*) or pretreated with 0.05% Me_2SO (*lanes 3* and *4*) or 10 μM Q3G (*lanes 5* and *6*) for 6 h prior to oxidative stress, as described under "Experimental Procedures." Both uncleaved precursor (110 kDa) and cleaved active (65 kDa) forms of SREBP-2 were visualized using an antibody that selectively recognizes SREBP-2. *C*, the quantified image after β-actin normalization is shown. Each *bar* represents the mean ± S.E. of two determinations from two independent experiments. *, $p < 0.05$ relative to H_2O_2-treated cells.

rat small intestine (43). A similar glucose transporter protein (GLUT1) is expressed in SH-SY5Y cells (44). A recent study has implicated GLUT1 in transporting the oxidized form of vitamin C to mitochondria in mammalian cells, thus conferring protection against oxidative damage (45). Hence, we hypothesize that a similar mechanism may be involved in the preferential uptake of Q3G by GLUT1 in SH-SY5Y cells, thereby protecting cells against oxidative damage.

Lipid peroxidation triggered by free radicals in isolated membrane is known to enhance formation of membrane-restricted cholesterol domains through self-associated cholesterol monomers (46). Similar to other flavonoids, the inhibition of lipid peroxidation by Q3G may be attributed to the presence of an *o*-dihydroxyl group (25). An additional mechanism for the cytoprotective effects of Q3G may be related to the ability of quercetin-like compounds to become intercalated between the acyl chains of phospholipids in the plasma membrane. The hydrophobic nature of quercetin and its ability to form π-π interactions with cholesterol may enable it to enter the lipid bilayer in a cholesterol-dependent fashion, resulting in resistance to lipid peroxidation (48). Conversely, membranes depleted of cholesterol display increased lipid peroxidation and an elevated loss of membrane integrity (49). Pretreatment with Q3G may therefore have produced cytoprotective effects by increasing the resistance of membranes to lipid peroxidation by increasing incorporation of this flavonoid into the plasma membrane.

Pretreatment of SH-SY5Y cells with Q3G followed by exposure to H_2O_2 reduced the loss of cellular viability and protected against necrotic cell death. Similarly, pretreatment of HEK293 and MCF-7 cells with a very low concentration of Q3G (0.1 μM) was effective in preventing the loss of cell viability produced by the H_2O_2 insult. Oxidative stress induced by H_2O_2 in bovine aortic endothelial cells has been shown to activate caspase-3 and increase the number of TUNEL-positive cells. In this study, ablation of lipid raft structure with methyl-β-cyclodextrin enhanced caspase-3 activation and TUNEL-positive cells in H_2O_2 treated cells, suggesting that cholesterol rich compartments mediate the prosurvival pathway under oxidative stress (9). In the present study, we did not observe a concordant reduction in H_2O_2-induced caspase-3 activation in cells pretreated with Q3G, suggesting that Q3G-mediated cytoprotection occurs by a caspase-3-independent pathway. This is contrary to several reports in which flavonoids have been shown to protect cells by inhibiting caspase-3 activation, loss of mitochondrial membrane potential, and the release of cytochrome *c* (37, 50, 51). Our observation is supported by a study in which quercetin

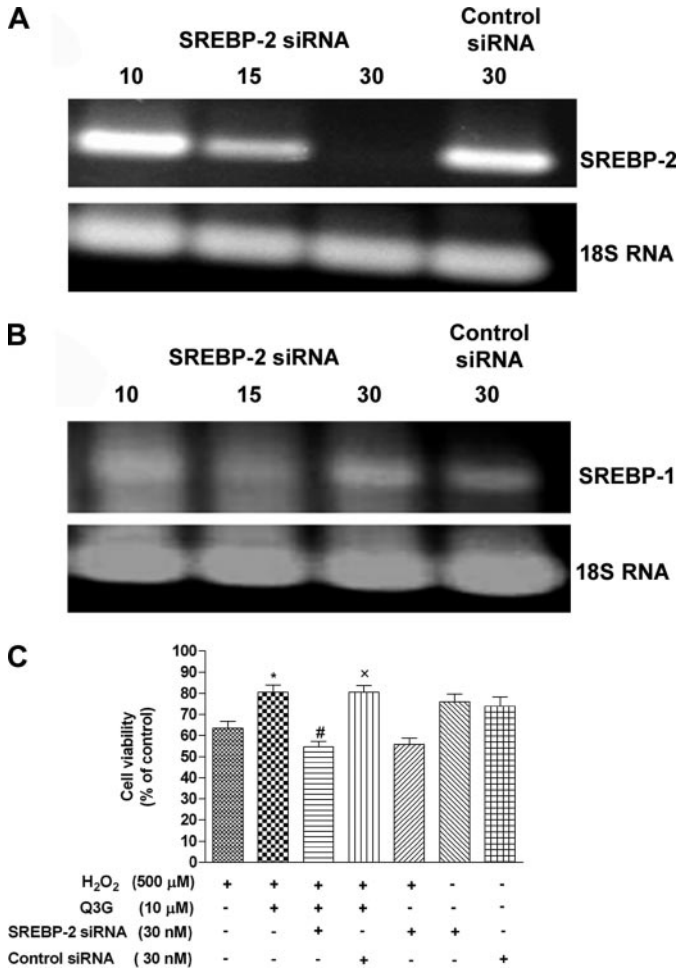

FIGURE 7. **siRNA-mediated knockdown of SREBP-2.** *A*, RT-PCR of SREBP-2 transcript. SH-SY5Y cells were transfected with varying concentration of siRNA-mediating knockdown of SREBP-2 (*lanes 1–3*) and 30 nM of control negative siRNA (*lane 4*) for 24 h. RT-PCR was performed using 100 ng of total RNA and specific primers for SREBP-2 and 18S as described under "Experimental Procedures." *B*, RT-PCR of SREBP-1 transcript. SH-SY5Y cells were transfected with varying concentrations of siRNA mediating knockdown of SREBP-2 (*lanes 1–3*) and 30 nM control siRNA (*lane 4*) for 24 h. RT-PCR was performed using 100 ng of total RNA and specific primers for SREBP-1 and 18S as described under "Experimental Procedures." *C*, SH-SY5Y cells were transfected with siRNA mediating knockdown of SREBP-2 (30 nM) and the negative control siRNA (30 nM) for 24 h. SH-SY5Y cells were pretreated with 0.05% Me_2SO or 10 μM Q3G for 6 h prior to the oxidative insult and placed in recovery media for 18 h. MTT assay was performed as described under "Experimental Procedures." Data are represented as percentage of cell viability of the untreated cells. Each *bar* represents the mean ± S.E. of 24 determinations from three independent experiments. *, $p < 0.05$ relative to all other groups, including H_2O_2-treated cells, except for the Q3G + H_2O_2 + control siRNA group, SREBP-2 siRNA group, and control siRNA group. #, **, $p < 0.01$ relative to all other group except H_2O_2 group and H_2O_2 + SREBP-2 siRNA group. ×, *, $p < 0.05$ relative to all other groups, including the +H_2O_2 only group, except for the Q3G + H_2O_2 group, SREBP-2 siRNA group, and control siRNA group.

metabolites also protected cardiomyoblasts against H_2O_2-induced oxidative stress by a caspase-3-independent pathway (52). We conclude that Q3G may protect SH-SY5Y cells against necrotic rather than apoptotic cell death.

A pivotal mechanism by which cells counteract oxidative stress is via the up-regulation of genes that encode antioxidant proteins, such as NQO1, NQO2, GST, HO-1 and γ-GCS (53, 54). In HepG2 cells, quercetin has been reported to enhance the Nrf2 (antioxidant-responsive element-nuclear factor-E2-related factor 2) pathway, leading to cytoprotection (55). Unlike quercetin, Q3G did not up-regulate these phase II antioxidant enzymes under oxidative stress in both SH-SY5Y and HEK293 cells. By contrast, we report a unique cytoprotective mechanism involving SREBP-2-mediated cholesterol biosynthesis only in Q3G-pretreated SH-SY5Y cells subjected to oxidative stress. Q3G pretreatment increased both the mRNA levels of SREBP-2 precursor and its processing into matured SREBP-2 under oxidative stress. In contrast, HEK 293 cells pretreated with Q3G showed a significant increase in SREBP-2 mRNA levels without a concomitant increase in SREBP-2 processing under oxidative stress. Similarly, in MCF-7 cells, Q3G failed to activate SREBP-2 signaling pathway. Since siRNA-mediated knockdown of SREBP-2 abolished Q3G-mediated cytoprotection, it appears that elevated SREBP-2 signaling is a protective mechanism unique to SH-SY5Y cells under oxidative stress. This finding is consistent with a study in which soy isoflavones were shown to increase the expression of a SRE-regulated gene by stimulating the maturation of SREBP-2 (56). The ability of Q3G pretreatment to activate SREBP-2 and elevate *de novo* synthesis of cholesterol only in cells under oxidative stress suggests that these events represent an adaptive response to cellular stress. These observations are supported by studies in fission yeast, where stress induced by hypoxia and heat shock led to increased SREBP-mediated transcription, resulting in *de novo* synthesis of cholesterol that compensated for the reduction in cholesterol levels produced by heat stress or low oxygen conditions (57). We propose that SREBP-2-mediated sterol synthesis protects against oxidative stress by decreasing lipid peroxidation, thereby maintaining membrane integrity.

A recent study also showed that treatment of HepG2 cells with a flavonoid, epigallocatechin gallate (EGCG), increased the active form of SREBP-2 (58). This elevation was attributed to inhibition of the ubiquitin-proteasome pathway by EGCG, resulting in a concomitant increase in SREBP-2 and LDLr activation (58). The mechanism by which Q3G increases SREBP-2 transcription and its processing is not known. We hypothesize that like another steroid-like analogue GW707 and the nonsteroidal molecules (GW300, GW532, and GW575), which are SCAP ligands, a structural analogue of Q3G derived from oxidative stress may also act as a SCAP ligand, thereby mediating cytoprotection via increased SREBP-2-induced gene expression (59).

Mevastatin, an inhibitor of HMG-CoA-reductase, blocks the synthesis of both nonsterol isoprenoids and sterols (60). We observed that mevastatin inhibited the protective effect of Q3G under oxidative stress, and this effect was reversed by the addition of IPP indicative of rescue of the mevalonate pathway. In the cholesterol synthesis pathway, OSC catalyzes the cyclization of monooxidosqualene to lanosterol (61). Since farnesylpyrophosphate is located upstream of OSC in the cholesterol synthesis pathway, inhibition of OSC should not block the formation of isoprenoids or affect protein prenylation or CoQ production. Consequently, blocking OSC would only inhibit sterol synthesis. Our finding that the OSCi blocked Q3G-me-

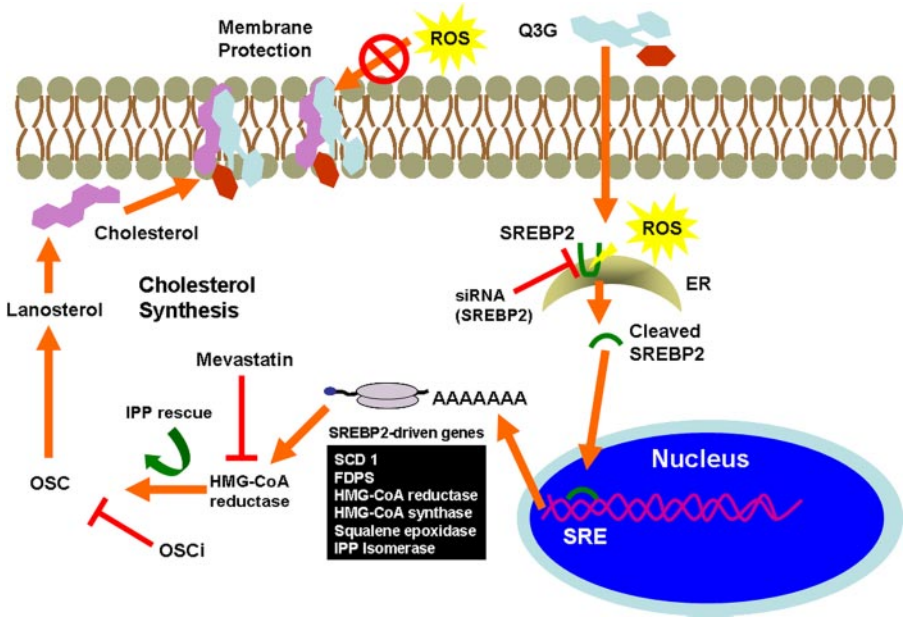

FIGURE 8. **Evidence for the proposed model for Q3G-mediated cytoprotection against oxidative stress.** Q3G reduces the loss of cellular viability produced by oxidative stress by decreasing levels of intracellular ROS in SH-SY5Y cells. In Q3G-primed cells, oxidative stress triggers the up-regulation of genes involved in cholesterol and lipid metabolism, leading to enhanced cholesterol synthesis. This reduces membrane damage by decreasing lipid peroxidation. Q3G pretreatment also induced the active form of SREBP-2 (65 kDa) and elevated the LDLr in cells under oxidative stress. siRNA-mediated knockdown of SREBP-2 abrogated the cytoprotective activity of Q3G, implicating SREBP-2 signaling in Q3G-induced cytoprotection. Inhibition of cholesterol and isoprenoid biosynthesis with mevastatin also blocked the cytoprotective effects of Q3G against oxidative stress-induced cell death. This latter effect was reversed by the addition of isopentenyl pyrophosphate, suggesting rescue of the mevalonate pathway. SH-SY5Y cells incubated with an OSCi reversed the protective effect of Q3G against oxidative stress, confirming the importance of cholesterol biosynthesis in Q3G-mediated cytoprotection. Last, Q3G-mediated cytoprotection was accompanied by enhanced incorporation of [^{14}C]acetate into [^{14}C]cholesterol. These findings suggest that cholesterol synthesis plays a key role in the adaptive response to oxidative stress following pretreatment with Q3G.

diated cytoprotection under oxidative stress suggested that Q3G-mediated cytoprotection involves sterol synthesis and not the nonsterol isoprenoids. Consistent with this result, the OSCi has been shown to block cholesterol synthesis in HepG2 cells in the nanomolar range (62). We analyzed *de novo* cholesterol synthesis using [^{14}C]acetate and found that Q3G pretreatment enhanced the incorporation of [^{14}C]acetate into [^{14}C]cholesterol under oxidative stress. The use of [^{14}C]acetate to study *de novo* synthesis of cholesterol is supported by numerous publications (63, 64). Taken together, these studies strongly suggest that elevated *de novo* cholesterol synthesis contributes to the cytoprotective effects of Q3G pretreatment in cells under oxidative stress.

Cholesterol depletion in cells leads to transcription of the LDLr gene that facilitates the uptake of LDL, a protein that aids in cholesterol transport. In contrast, excess cholesterol represses LDLr expression. The expression of LDLr is regulated by SREBPs (65). In the present study, we show increased LDLr expression by Q3G pretreatment in cells under oxidative stress. In concordance with these findings, several compounds, including curcumin and polyphenols present in red grape juice have been shown to activate LDLr expression, thereby reducing circulating levels of cholesterol (66, 67). The fact that LDLr expression was elevated in Q3G-treated cells under oxidative stress suggests that a similar mechanism may also apply to this flavonoid. This mechanism is compatible with the ability of Q3G to protect SH-SY5Y cells by *de novo* cholesterol synthesis.

Several studies have demonstrated the induction of cholesterol efflux by flavonoids (47, 68). Anthocyanin-induced chlolesterol efflux from mouse peritoneal macrophages and macrophage-derived foam cells is mediated in part by the peroxisome proliferator-activated receptor γ-LXRα-ABCA1 pathway (47). SH-SY5Y cells pretreated with Q3G did not show an increase in cholesterol efflux under oxidative stress (data not shown). Moreover, Q3G did not induce transcriptional activation of LXRα (data not shown), indicating that cholesterol efflux did not account for the increase in cholesterol synthesis induced by Q3G in cells under oxidative stress.

Based on our findings, we propose a novel model for Q3G-mediated cytoprotection against oxidative stress (Fig. 8). In this model, Q3G, a flavonol abundant in apple skins, protects SH-SY5Y cells against H_2O_2-induced oxidative stress by the up-regulation of genes involved in cholesterol synthesis. Elevated synthesis of cholesterol by Q3G serves to protect SH-SY5Y cells from oxidative stress by reducing lipid peroxidation and membrane damage. A logical extension of our studies would be to use appropriate animal disease models to determine if Q3G may be useful in the treatment of cardiovascular and neurodegenerative diseases by a similar mechanism.

Acknowledgments—We thank the South Alberta Microarray Facility at Calgary, especially Dr. Xiuling Wang, for conducting the microarray experiments. We thank Dr. Barbara Karten for critical reading of the manuscript. We greatly acknowledge Dr. Harold A. Robertson for the use of quantitative RT-PCR and microarray facilities. We thank Drs. Robert Gilbert and Xiangfeng Sun for technical advice on microarray. Dr. Andrea Hebb is acknowledged for assistance with quantitative RT-PCR.

REFERENCES

1. Yeagle, P. L. (1985) *Biochim. Biophys. Acta* **822,** 267–287
2. Yeagle, P. L. (1991) *Biochimie* (*Paris*) **73,** 1303–1310
3. Incardona, J. P., and Eaton, S. (2000) *Curr. Opin. Cell Biol.* **12,** 193–203
4. Zhuang, L., Kim, J., Adam, R. M., Solomon, K. R., and Freeman, M. R. (2005) *J. Clin. Invest.* **115,** 959–968
5. Goldstein, J. L., and Brown, M. S. (1990) *Nature* **343,** 425–430
6. Brown, M. S., and Goldstein, J. L. (1997) *Cell* **89,** 331–340
7. Goldstein, J. L., DeBose-Boyd, R. A., and Brown, M. S. (2006) *Cell* **124,** 35–46
8. Yang, T., Espenshade, P. J., Wright, M. E., Yabe, D., Gong, Y., Aebersold,

R., Goldstein, J. L., and Brown, M. S. (2002) *Cell* **110,** 489–500
9. Yang, B., Oo, T. N., and Rizzo, V. (2006) *FASEB J.* **20,** 1501–1503
10. Chance, B., Sies, H., and Boveris, A. (1979) *Physiol. Rev.* **59,** 527–605
11. Ames, B. N. (1983) *Science* **221,** 1256–1264
12. Halliwell, B. (1993) *Haemostasis* **23,** Suppl. 1, 118–126
13. Yagi, K. (1987) *Chem. Phys. Lipids* **45,** 337–351
14. Girotti, A. W. (1998) *J. Lipid Res.* **39,** 1529–1542
15. Gutteridge, J. M., and Halliwell, B. (2000) *Ann. N. Y. Acad. Sci.* **899,** 136–147
16. Montine, K. S., Quinn, J. F., Zhang, J., Fessel, J. P., Roberts, L. J., Morrow, J. D., and Montine, T. J. (2004) *Chem. Phys. Lipids* **128,** 117–124
17. Halliwell, B. (2006) *J. Neurochem.* **97,** 1634–1658
18. Gilgun-Sherki, Y., Rosenbaum, Z., Melamed, E., and Offen, D. (2002) *Pharmacol. Rev.* **54,** 271–284
19. Itoh, K., Chiba, T., Takahashi, S., Ishii, T., Igarashi, K., Katoh, Y., Oyake, T., Hayashi, N., Satoh, K., Hatayama, I., Yamamoto, M., and Nabeshima, Y. (1997) *Biochem. Biophys. Res. Commun.* **236,** 313–322
20. Sies, H. (1997) *Exp. Physiol.* **82,** 291–295
21. Youdim, K. A., Spencer, J. P., Schroeter, H., and Rice-Evans, C. (2002) *Biol. Chem.* **383,** 503–519
22. Boyer, J., and Liu, R. H. (2004) *Nutr. J.* **3,** 1–15
23. Spencer, J. P., Abd-el-Mohsen, M. M., and Rice-Evans, C. (2004) *Arch. Biochem. Biophys.* **423,** 148–161
24. Williams, R. J., Spencer, J. P., and Rice-Evans, C. (2004) *Free Radic. Biol. Med.* **36,** 838–849
25. Peng, I. W., and Kuo, S. M. (2003) *J. Nutr.* **133,** 2184–2187
26. Molina, M. F., Sanchez-Reus, I., Iglesias, I., and Benedi, J. (2003) *Biol. Pharm. Bull.* **26,** 1398–1402
27. Dajas, F., Rivera-Megret, F., Blasina, F., Arredondo, F., Abin-Carriquiry, J. A., Costa, G., Echeverry, C., Lafon, L., Heizen, H., Ferreira, M., et al. (2003) *Braz. J. Med. Biol. Res.* **36,** 1613–1620
28. Mandel, S., Amit, T., Reznichenko, L., Weinreb, O., and Youdim, M. B. (2006) *Mol. Nutr. Food Res.* **50,** 229–234
29. Youdim, K. A., Shukitt-Hale, B., and Joseph, J. A. (2004) *Free Radic. Biol. Med.* **37,** 1683–1693
30. Frolov, A., Zielinski, S. E., Crowley, J. R., Dudley-Rucker, N., Schaffer, J. E., and Ory, D. S. (2003) *J. Biol. Chem.* **278,** 25517–25525
31. Yang, Y. H., Dudoit, S., Luu, P., Lin, D. M., Peng, V., Ngai, J., and Speed, T. P. (2002) *Nucleic Acids Res.* **30,** 1–10
32. Wang, J., Yu, L., Schmidt, R. E., Su, C., Huang, X., Gould, K., and Cao, G. (2005) *Biochem. Biophys. Res. Commun.* **332,** 735–742
33. Skarits, C., Fischer, S., and Haas, O. A. (2003) *Clin. Chim. Acta* **336,** 27–37
34. Livak, K. J., and Schmittgen, T. D. (2001) *Methods* **25,** 402–408
35. Singh, D. K., and Porter, T. D. (2006) *J. Nutr.* **136,** 759S–764S
36. Ayala-Grosso, C., Ng, G., Roy, S., and Robertson, G. S. (2002) *Brain Pathol.* **12,** 430–441
37. Choi, Y. J., Jeong, Y. J., Lee, Y. J., Kwon, H. M., and Kang, Y. H. (2005) *J. Nutr.* **135,** 707–713
38. Jeong, Y. J., Choi, Y. J., Kwon, H. M., Kang, S. W., Park, H. S., Lee, M., and Kang, Y. H. (2005) *Br. J. Nutr.* **93,** 581–591
39. Chow, J. M., Shen, S. C., Huan, S. K., Lin, H. Y., and Chen, Y. C. (2005) *Biochem. Pharmacol.* **69,** 1839–1851
40. Wang, H., and Joseph, J. A. (1999) *Free Radic. Biol. Med.* **27,** 683–694
41. Ishige, K., Schubert, D., and Sagara, Y. (2001) *Free Radic. Biol. Med.* **30,** 433–446
42. Williamson, G., Plumb, G. W., Uda, Y., Price, K. R., and Rhodes, M. J. (1996) *Carcinogenesis* **17,** 2385–2387
43. Wolffram, S., Block, M., and Ader, P. (2002) *J. Nutr.* **132,** 630–635
44. Russo, V. C., Kobayashi, K., Najdovska, S., Baker, N. L., and Werther, G. A. (2004) *Brain Res.* **1009,** 40–53
45. KC, S., Carcamo, J. M., and Golde, D. W. (2005) *FASEB J.* **19,** 1657–1667
46. Jacob, R. F., and Mason, R. P. (2005) *J. Biol. Chem.* **280,** 39380–39387
47. Xia, M., Hou, M., Zhu, H., Ma, J., Tang, Z., Wang, Q., Li, Y., Chi, D., Yu, X., Zhao, T., Han, P., Xia, X., and Ling, W. (2005) *J. Biol. Chem.* **280,** 36792–36801
48. Saija, A., Scalese, M., Lanza, M., Marzullo, D., Bonina, F., and Castelli, F. (1995) *Free Radic. Biol. Med.* **19,** 481–486
49. Lopez-Revuelta, A., Sanchez-Gallego, J. I., Hernandez-Hernandez, A., Sanchez-Yague, J., and Llanillo, M. (2006) *Chem. Biol. Interact.* **161,** 79–91
50. Kang, S. S., Lee, J. Y., Choi, Y. K., Kim, G. S., and Han, B. H. (2004) *Bioorg. Med. Chem. Lett.* **14,** 2261–2264
51. Shin, D. H., Bae, Y. C., Kim-Han, J. S., Lee, J. H., Choi, I. Y., Son, K. H., Kang, S. S., Kim, W. K., and Han, B. H. (2006) *J. Neurochem.* **96,** 561–572
52. Angeloni, C., Spencer, J. P., Leoncini, E., Biagi, P. L., and Hrelia, S. (2007) *Biochimie* (*Paris*) **89,** 73–82
53. Dhakshinamoorthy, S., Long, D. J., and Jaiswal, A. K. (2000) *Curr. Top. Cell Regul.* **36,** 201–216
54. Jaiswal, A. K. (2004) *Free Radic. Biol. Med.* **36,** 1199–1207
55. Tanigawa, S., Fujii, M., and Hou, D. X. (2007) *Free Radic. Biol. Med.* **42,** 1690–1703
56. Mullen, E., Brown, R. M., Osborne, T. F., and Shay, N. F. (2004) *J. Nutr.* **134,** 2942–2947
57. Robichon, C., and Dugail, I. (2007) *Biochimie* (*Paris*) **89,** 260–264
58. Kuhn, D. J., Burns, A. C., Kazi, A., and Dou, Q. P. (2004) *Biochim. Biophys. Acta* **1682,** 1–10
59. Grand-Perret, T., Bouillot, A., Perrot, A., Commans, S., Walker, M., and Issandou, M. (2001) *Nat. Med.* **7,** 1332–1338
60. Endo, A. (2004) *Atheroscler. Suppl.* **5,** 67–80
61. Cattel, L., Ceruti, M., Viola, F., Delprino, L., Balliano, G., Duriatti, A., and Bouvier-Nave, P. (1986) *Lipids* **21,** 31–38
62. Morand, O. H., Aebi, J. D., Dehmlow, H., Ji, Y. H., Gains, N., Lengsfeld, H., and Himber, J. (1997) *J. Lipid Res.* **38,** 373–390
63. Beyea, M. M., Heslop, C. L., Sawyez, C. G., Edwards, J. Y., Markle, J. G., Hegele, R. A., and Huff, M. W. (2007) *J. Biol. Chem.* **282,** 5207–5216
64. Higashi, Y., Itabe, H., Fukase, H., Mori, M., Fujimoto, Y., and Takano, T. (2003) *J. Biol. Chem.* **278,** 21450–21458
65. Brown, M. S., and Goldstein, J. L. (1999) *Proc. Natl. Acad. Sci. U. S. A.* **96,** 11041–11048
66. Fan, C., Wo, X., Dou, X., Xu, L., Qian, Y., Luo, Y., and Yan, J. (2006) *Pharmacol. Rep* **58,** 577–581
67. Davalos, A., Fernandez-Hernando, C., Cerrato, F., Martinez-Botas, J., Gomez-Coronado, D., Gomez-Cordoves, C., and Lasuncion, M. A. (2006) *J. Nutr.* **136,** 1766–1773
68. Bursill, C. A., and Roach, P. D. (2006) *J. Agric. Food Chem.* **54,** 1621–1626

Quercetin 3-Glucoside Protects Neuroblastoma (SH-SY5Y) Cells *in Vitro* against Oxidative Damage by Inducing Sterol Regulatory Element-binding Protein-2-mediated Cholesterol Biosynthesis

Ramani Soundararajan, Alexander D. Wishart, H. P. Vasantha Rupasinghe, Mayi Arcellana-Panlilio, Carolanne M. Nelson, Michael Mayne and George S. Robertson

J. Biol. Chem. 2008, 283:2231-2245.
doi: 10.1074/jbc.M703583200 originally published online November 20, 2007
